

A SUBSTRUCTURING PRECONDITIONER WITH VERTEX-RELATED INTERFACE SOLVERS FOR ELLIPTIC-TYPE EQUATIONS IN THREE DIMENSIONS

QIYA HU AND SHAOLIANG HU

ABSTRACT. In this paper we propose a variant of the substructuring preconditioner for solving three-dimensional elliptic-type equations with strongly discontinuous coefficients. In the proposed preconditioner, we use the simplest coarse solver associated with the finite element space induced by the coarse partition, and construct inexact interface solvers based on overlapping domain decomposition with small overlaps. This new preconditioner has an important merit: its construction and efficiency do not depend on the concrete form of the considered elliptic-type equations. We apply the proposed preconditioner to solve the linear elasticity problems and Maxwell's equations in three dimensions. Numerical results show that the convergence rate of PCG method with the preconditioner is nearly optimal, and also robust with respect to the (possibly large) jumps of the coefficients in the considered equations.

Keywords: domain decomposition, substructuring preconditioner, linear elasticity problems, Maxwell's equations, PCG iteration, convergence rate

AMS subject classifications. 65N30, 65N55.

1. INTRODUCTION

There are many works to study domain decomposition methods (DDMs) for solving the systems generated by finite element discretization of elliptic-type partial differential equations ([1]-[5],[7]-[24], [27]-[42], [46]-[48], [50]-[51],[49, 53] and the references therein). It is known that, for three dimensional problems, non-overlapping domain decomposition methods (DDMs) are more difficult to construct and implement than overlapping DDMs although the non-overlapping DDMs have some advantages over the overlapping DDMs in the treatment of jump coefficients. In fact, the construction of non-overlapping DDMs heavily depends on the considered models in three dimensiona. For example, non-overlapping DDMs for positive definite Maxwell's equations are essentially different from the usual elliptic equation (comparing [13, 30, 32, 48]). This drawbacks restrict applications of the non-overlapping DDMs.

1. LSEC, ICMSEC, Academy of Mathematics and Systems Science, Chinese Academy of Sciences, Beijing 100190, China; 2. School of Mathematical Sciences, University of Chinese Academy of Sciences, Beijing 100049, China (hxy@lsec.cc.ac.cn and hushaoliang@lsec.cc.ac.cn). This work was funded by Natural Science Foundation of China G11571352.

A key ingredient in the construction of non-overlapping domain decomposition methods is the choice of a suitable coarse subspace. There are two main ways to construct coarse subspaces in the existing works: (i) use some degrees of freedom on the *joint-set* (BPS method, FETI-DP method, BDDC method); (ii) use the local kernel spaces of the considered differential operator (Neumann-Neumann method, BDD method, FETI method). But, there are some drawbacks in the two ways. For the first way, the choice of degrees of freedom heavily depends on the considered model, for example, one can choose the degrees of freedom on the vertices, the averages on the edges or faces for the three dimensional Laplace equation, but this choice is not practical for the three dimensional Maxwell's equations (see [13], [31], [32] and [48]). For the second way, the coarse space may be very large. For example, the kernel space of the *curl* operator is just the gradient of the nodal finite element space, so (by simple calculation) the dimensions of such coarse space for Maxwell's equations are greater than $1/7$ of that of the original solution space.

Another possible choice of coarse subspace is the finite element space induced by the coarse partition. This coarse subspace was first considered in [15] for elliptic equations, and then was investigated in [53]. It is clear that this coarse subspace possesses the simplest structure and almost the smallest degrees of freedom among the coarse subspaces considered in the existing non-overlapping DDMS for three-dimensional problems. However, such coarse subspace was regarded as a unapplicable coarse subspace for long time, since the condition number of the resulting preconditioned system is not nearly optimal for three dimensional problems with large jump coefficients. For elliptic equations in three dimensions, substructuring preconditioners with such coarse subspace was studied again in [29]. Based on the framework developed in [52], it was shown that the PCG method for solving the resulting preconditioned system has the nearly stable convergence even for the case with large jump coefficients. In [30], this kind of coarse solver was also applied to the construction of substructuring preconditioner for Maxwell's equations in three dimensions. Unfortunately, for this choice of coarse subspace, we need to design local interface solvers on coarse edges, whose definitions still depend on the considered models (comparing [30] with [29]).

In the present paper, we try to construct relatively united substructuring preconditioner for elliptic-type equations, such that it is cheap, easy to implement and has fast convergence. As usual, we decompose the considered domain into the union of some non-overlapping subdomains, which constitute a coarse partition of the domain. In the proposed preconditioner, we use the simplest coarse space induced by the coarse partition (see [15], [29], [30] and [53]). The main goal of this paper is to design unified and practical local interface solvers.

For each internal cross-point, we introduce an auxiliary subdomain that contains the internal cross-point as its "center" and has almost the same size with the original

subdomains. Associated with each auxiliary subdomain, we define a local interface solver such that the solution of the local interface problem is discrete harmonic in the intersection of the auxiliary subdomain with every original subdomain adjoining to it. Notice that each intersection is only a part of some original subdomain, so the local interface solver corresponds to “inexact” harmonic extensions. Such a local interface solver is implemented by solving a Dirichlet problem (residual equation), which is defined on the natural restriction space of the original finite element space on the auxiliary subdomain. It is clear that each local interface solver has almost the same cost with an original subdomain solver. We point out that the proposed local interface solvers are different from the existing local interface solvers defined in the vertex space method [46] or the interface overlapping additive Schwarz [53], where exact harmonic extensions are required.

In order to further reduce the cost of the local interface solvers described above, we present approximate local interface solvers based on a coarsening technique. In the step for solving a local interface problem, we are interested only in the degrees of freedom on the local interface, instead of the degrees of freedom in the interiors of subdomains. Intuitively, the accuracy of the degrees of freedom on the local interface are not sensitive to the grids far from the local interface. Based on this observation, we construct auxiliary non-uniform grids in each subdomain adjoining the considered local interface such that the auxiliary grids coincide with the original fine grids on the local interface but gradually become coarser when nodes are far from the local interface. The desired approximate local interface solver is implemented by solving a Dirichlet problem on the finite element space defined by the auxiliary grids, which have much smaller nodes than the original fine grids.

The constructions of the coarse solver and the proposed local interface solvers do not depend on the considered models, and the resulting substructuring preconditioner is cheap and easy to implement. As pointed out in [13], the design of an efficient substructuring preconditioner for three dimensional Maxwell’s equations poses quite significant challenges. A few existing preconditioners on this topic are either expensive or difficult to implement. We will apply the proposed substructuring preconditioner to solve the linear elasticity problems and Maxwell’s equations in three dimensions. Numerical results show that the preconditioner is robust uniformly for the two kinds of equations even if the coefficients have large jumps. We also consider possible extension of the preconditioner to the case with irregular subdomains.

The outline of the paper is as follows. In Section 2, we give the variational formula of general elliptic-type equations and introduce a partition based on domain decomposition. In Section 3, we describe local interface solvers associated with vertex-related subdomains and define the resulting substructuring preconditioner for the general elliptic system. In Section 4, we present an analysis of convergence

of the preconditioner for linear elasticity problems. In section 5, we will report the some numerical results for the linear elasticity problems and Maxwell's equations.

2. ELLIPTIC-TYPE EQUATIONS AND DOMAIN DECOMPOSITION

In this section, we describe the considered problems.

2.1. Elliptic-type equations. Let Ω be a bounded and connected Lipschitz domain in \mathbb{R}^3 . For convenience, we just consider the weak form of elliptic-type equations. Let $V(\Omega)$ denote a Hilbert space with the scalar product $(\cdot, \cdot)_V$, and $\|\cdot\|_V$ be the induced norm. We introduce a real bilinear form $\mathcal{A}(\cdot, \cdot) : V(\Omega) \times V(\Omega) \rightarrow \mathbb{R}$. We assume that $\mathcal{A}(\cdot, \cdot)$ is symmetric,

$$\mathcal{A}(\mathbf{u}, \mathbf{v}) = \mathcal{A}(\mathbf{v}, \mathbf{u}), \quad \mathbf{u}, \mathbf{v} \in V(\Omega)$$

continuous,

$$|\mathcal{A}(\mathbf{u}, \mathbf{v})| \leq c_1 \|\mathbf{u}\|_V \|\mathbf{v}\|_V, \quad \mathbf{u}, \mathbf{v} \in V(\Omega) \quad c_1 > 0$$

and coercive

$$\mathcal{A}(\mathbf{u}, \mathbf{u}) \geq c_2 \|\mathbf{u}\|_V^2, \quad \mathbf{u} \in V(\Omega), \quad c_2 > 0.$$

Given a linear functional $\mathbf{F} \in V'(\Omega)$, we consider the following problem:

$$\begin{cases} \text{Find } \mathbf{u} \in V(\Omega) & .st. \\ \mathcal{A}(\mathbf{u}, \mathbf{v}) = (\mathbf{F}, \mathbf{v}), & \forall \mathbf{v} \in V(\Omega), \end{cases} \quad (2.1)$$

where (\cdot, \cdot) denotes the duality pairing between $V'(\Omega)$ and $V(\Omega)$.

2.2. Domain decomposition and discretization. For convenience, we assume that Ω is a polyhedra. For a number $d \in (0, 1)$, let Ω be decomposed into the union of non-overlapping tetrahedra (or hexahedra) $\{\Omega_k\}$ with the size d . Then, we get a non-overlapping domain decomposition for Ω : $\bar{\Omega} = \bigcup_{k=1}^N \bar{\Omega}_k$. Assume that $\Omega_i \cap \Omega_j = \emptyset$ when $i \neq j$; if $i \neq j$ and $\partial\Omega_i \cap \partial\Omega_j \neq \emptyset$, then $\partial\Omega_i \cap \partial\Omega_j$ is a common face of Ω_i and Ω_j , or a common edge of Ω_i and Ω_j , or a common vertex of Ω_i and Ω_j . It is clear that the subdomains $\Omega_1, \dots, \Omega_N$ constitute a *coarse* partition \mathcal{T}_d of Ω . If $\partial\Omega_i \cap \partial\Omega_j$ is just a common face of Ω_i and Ω_j , then set $\Gamma_{ij} = \partial\Omega_i \cap \partial\Omega_j$. Define $\Gamma = \cup \Gamma_{ij}$. By Γ_k we denote the intersection of Γ with the boundary of the subdomain Ω_k . So we have $\Gamma_k = \partial\Omega_k$ if Ω_k is an interior subdomain of Ω .

With each subdomain Ω_k we associate a regular triangulation made of tetrahedral elements (or hexahedral elements). We require that the triangulations in the subdomains match on the interfaces between subdomains, and so they constitute a triangulation \mathcal{T}_h on the domain Ω , which we assume is quasi-uniform. We denote by h the mesh size of \mathcal{T}_h , i.e., h denotes the maximum diameter of tetrahedra in the mesh \mathcal{T}_h .

For an element $K \in \mathcal{T}_h$, let $R(K)$ denote a set of basis functions on the element K . The definition of $R(K)$ depends on the considered models, and will be given in Section 4.2 and Subsection 5.2. Define the finite element space

$$V_h(\Omega) = \left\{ \mathbf{v} \in V(\Omega) : \mathbf{v}|_K \in R(K), \forall K \in \mathcal{T}_h \right\},$$

Consider the discrete problem of (2.1): *Find $\mathbf{u}_h \in V_h(\Omega)$ such that*

$$\mathcal{A}(\mathbf{u}_h, \mathbf{v}) = (\mathbf{F}, \mathbf{v}), \quad \forall \mathbf{v} \in V_h(\Omega). \quad (2.2)$$

This is the whole problem we need to solve in this paper.

For convenience, we define the discrete operator $A : V_h(\Omega) \rightarrow V_h(\Omega)$ as

$$(A\mathbf{u}, \mathbf{v}) = \mathcal{A}(\mathbf{u}, \mathbf{v}), \quad \mathbf{u}, \mathbf{v} \in V_h(\Omega).$$

Then (2.2) can be written in the operator form

$$A\mathbf{u}_h = \mathbf{f}. \quad (2.3)$$

By the assumptions on $\mathcal{A}(\cdot, \cdot)$, the operator is symmetric and positive definite. Thus the above equation can be iteratively solved by CG method. In the rest of this paper, we will construct a preconditioner for the operator A .

Before constructing the desired preconditioner, we first introduce some useful sets and subspaces.

\mathcal{N}_h : the set of all nodes generated by the *fine* partition \mathcal{T}_h ;

\mathcal{E}_h : the set of all *fine* edges generated by the partition \mathcal{T}_h ;

\mathcal{F}_h : the set of all *fine* faces generated by the partition \mathcal{T}_h ;

\mathcal{N}_d : the set of all nodes generated by the *coarse* partition \mathcal{N}_d .

In most applications, the degrees of freedom of $\mathbf{v} \in V_h(\Omega)$ are defined at the nodes in \mathcal{N}_h (the nodal elements), or on the edges in \mathcal{E}_h (Nedelec edge elements), or on the faces in \mathcal{F}_h (Raviart-Thomas face elements). Throughout this paper, for a subset F that is the union of faces in \mathcal{F}_h , the term “the degrees of freedom of \mathbf{v} vanish on F ” means that “ \mathbf{v} has the zero degrees of freedom at the nodes, or fine edges, or fine faces of F ”.

Let $G \subset \Omega$ be a subdomain that is the union of some elements in \mathcal{T}_h . Define

$$V_h^0(G) = \{v \in V_h(\Omega) : \text{the degrees of freedom of } \mathbf{v} \text{ vanish on } \partial G\}.$$

For example, when $G = \Omega_k$ the space $V_h^0(\Omega_k)$ is just the subdomain space in the traditional substructuring methods.

For the construction of the desired preconditioner, we will use the simplest coarse space $V_d(\Omega)$, which is defined as the finite element space associated with the *coarse* partition \mathcal{T}_d (see [15], [29], [30] and [53]). It is clear that $V_d(\Omega) \subset V_h(\Omega)$.

3. A PRECONDITIONER WITH VERTEX-RELATED LOCAL INTERFACE SOLVERS

This section is devoted to describing the desired preconditioner, in which local interface solvers are defined in vertex-related subspaces.

3.1. Space decomposition. For each $v \in \mathcal{N}_d$, we construct an open region Ω_V^{half} , whose “center” is v and size is about d , see Figure 1. When $v \in \partial\Omega$, the auxiliary subdomain Ω_V^{half} is chosen as the part in Ω . We assume that: (i) each subdomain Ω_V^{half} is just the union of some elements in \mathcal{T}_h ; (ii) the union of all the interface subdomains $\Omega_V^{half} \cap \Gamma$ is an open cover of Γ . Then all the interface subdomains $\Omega_V^{half} \cap \Gamma$ constitute an overlapping domain decomposition of Γ (with small overlap), where the overlap can be one element layer only. Here we do not require that all the subdomains Ω_V^{half} constitute an overlapping domain decomposition of the original domain Ω , so we can choose slightly smaller subdomains Ω_V^{half} in applications.

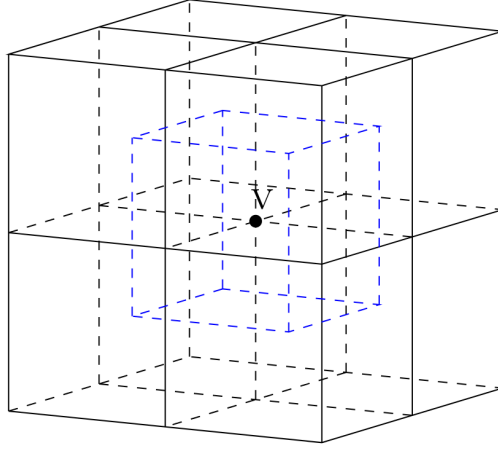


FIGURE 1. The auxiliary subdomain Ω_V^{half} (the blue cube) associated with the vertex v .

In order to define a space decomposition of $V_h(\Omega)$ in an exact manner, we need to introduce more notations.

For $v \in \mathcal{N}_d$, set

$$\Lambda_V = \{k : \text{the polyhedron } \Omega_k \text{ contains } v \text{ as its vertex}\}$$

and define

$$\Gamma_V^{half} = \Omega_V^{half} \cap \Gamma \text{ and } \Omega_V = \bigcup_{k \in \Lambda_V} \Omega_k.$$

Let $V_h(\Gamma)$ denote the interface space, which consists of the natural traces of all the functions in $V_h(\Omega)$. Define the vertex-related local interface space

$$V_h^0(\Gamma_V^{half}) = \{\phi \in V_h(\Gamma) : \text{supp } \phi \subset \Gamma_V^{half}\}.$$

Since all the vertex-related local interfaces Γ_V^{half} constitute an open cover of the interface Γ , we have the space decomposition

$$V_h(\Gamma) = \bigcup_{V \in \mathcal{N}_d} V_h^0(\Gamma_V^{half}). \quad (3.1)$$

As usual, let $V_h^\perp(\Omega)$ denote the space consisting of all the finite element functions that are discrete harmonic in each Ω_k , namely

$$V_h^\perp(\Omega) = \{\mathbf{v} \in V_h(\Omega) : \mathcal{A}(\mathbf{v}, \mathbf{w}) = 0, \forall \mathbf{w} \in V_h^0(\Omega_k) \text{ for each } \Omega_k\}.$$

For each $v \in \mathcal{N}_d$, define vertex-related local harmonic space

$$V_h^\perp(\Omega_V) = \{\mathbf{v} \in V_h^\perp(\Omega) : \text{the trace of } \mathbf{v} \text{ belongs to } V_h^0(\Gamma_V^{half})\} \subset V_h^0(\Omega_V).$$

In other words, $V_h^\perp(\Omega_V)$ is just the space consisting of the discrete harmonic extensions of the functions in $V_h^0(\Gamma_V^{half})$.

It is clear that

$$V_h^\perp(\Omega) = \bigcup_{V \in \mathcal{N}_d} V_h^\perp(\Omega_V).$$

Thus the space $V_h(\Omega)$ admits the space decomposition

$$V_h(\Omega) = V_d(\Omega) + \sum_{k=1}^N V_h^0(\Omega_k) + \sum_{V \in \mathcal{N}_d} V_h^\perp(\Omega_V). \quad (3.2)$$

3.2. Preconditioner. In this subsection we define solvers on the subspaces $V_d(\Omega)$, $V_h^0(\Omega_k)$ and $V_h^\perp(\Omega_V)$.

As usual, we use $A_d : V_d(\Omega) \rightarrow V_d(\Omega)$ and $A_k : V_h^0(\Omega_k) \rightarrow V_h^0(\Omega_k)$ to denote the restriction of A on $V_d(\Omega)$ and $V_h^0(\Omega_k)$ respectively, i.e., they satisfy

$$(A_d \mathbf{v}_d, \mathbf{w}_d) = \mathcal{A}(\mathbf{v}_d, \mathbf{w}_d), \quad \mathbf{v}_d \in V_d(\Omega), \quad \forall \mathbf{w}_d \in V_d(\Omega)$$

and

$$(A_k \mathbf{v}, \mathbf{w})_{\Omega_k} = (A \mathbf{v}, \mathbf{w}) = \mathcal{A}(\mathbf{v}, \mathbf{w}), \quad \mathbf{v} \in V_h^0(\Omega_k), \quad \forall \mathbf{w} \in V_h^0(\Omega_k).$$

In the following we define an ‘‘inexact’’ solver on $V_h^\perp(\Omega_V)$. To this end, we introduce a modification of $V_h^\perp(\Omega_V)$. Let $k \in \Lambda_V$, and use $\Omega_{V,k}^{half}$ to denote the intersection of Ω_V^{half} with Ω_k . For each $\Omega_{V,k}^{half}$, define the ‘‘inexact’’ harmonic space

$$V_h^\perp(\Omega_V^{half}) = \{\mathbf{v} \in V_h^0(\Omega_V^{half}) : \mathcal{A}(\mathbf{v}, \mathbf{w}) = 0, \forall \mathbf{w} \in V_h^0(\Omega_{V,k}^{half}) \text{ with } k \in \Lambda_V\}.$$

Notice that the functions in $V_h^\perp(\Omega_V^{half})$ have the support set Ω_V^{half} and are harmonic only in the subdomain $\Omega_{V,k}^{half}$ of Ω_k (for any $k \in \Lambda_V$).

For a function $\mathbf{v} \in V_h^\perp(\Omega_V)$, define $\mathbf{v}^{half} \in V_h^\perp(\Omega_V^{half})$ such that $\mathbf{v}^{half} = \mathbf{v}$ on Γ_V^{half} . For each $v \in \mathcal{N}_d$, let $B_V : V_h^\perp(\Omega_V) \rightarrow V_h^\perp(\Omega_V)$ be the symmetric and positive definite operator defined by

$$(B_V \mathbf{v}, \mathbf{w}) = \mathcal{A}(\mathbf{v}^{half}, \mathbf{w}^{half}), \quad \mathbf{v} \in V_h^\perp(\Omega_V), \quad \forall \mathbf{w} \in V_h^\perp(\Omega_V).$$

Since the basis functions in $V_h^\perp(\Omega_V)$ are not known, the action of B_V^{-1} needs to be implemented by solving a residual equation defined in $V_h^0(\Omega_V^{half})$ (see **Algorithm 3.1** given later).

Let $Q_d : V_h(\Omega) \rightarrow V_d(\Omega)$, $Q_k : V_h(\Omega) \rightarrow V_h^0(\Omega_k)$ and $Q_V : V_h(\Omega) \rightarrow V_h^\perp(\Omega_V)$ be the standard L^2 -projectors. Then the preconditioner for A is defined as follows:

$$B^{-1} = A_d^{-1}Q_d + \sum_{k=1}^N A_k^{-1}Q_k + \sum_{V \in \mathcal{N}_d} B_V^{-1}Q_V \quad (3.3)$$

The action of the preconditioner B^{-1} , which is needed in each iteration step of PCG method, can be described by the following algorithm.

Algorithm 3.1. For $\mathbf{g} \in V_h(\Omega)$, we can compute $\mathbf{u} = B^{-1}\mathbf{g}$ in four steps.

Step 1. Solve the system for $\mathbf{u}_d \in V_d(\Omega)$:

$$(A_d \mathbf{u}_d, \mathbf{v}_d) = (\mathbf{g}, \mathbf{v}_d), \quad \forall \mathbf{v}_d \in V_d(\Omega);$$

Step 2. Solve the following system for $\mathbf{u}_k \in V_h^0(\Omega_k)$ ($k = 1, \dots, N$) in parallel:

$$(A_k \mathbf{u}_k, \mathbf{v}) = (\mathbf{g}, \mathbf{v}), \quad \forall \mathbf{v} \in V_h^0(\Omega_k), \quad k = 1, \dots, N;$$

Step 3. Solve the following system for $\mathbf{u}_V \in V_h^0(\Omega_V^{half})$ ($V \in \mathcal{N}_d$) in parallel:

$$(B_V \mathbf{u}_V, \mathbf{v}) = (\mathbf{g}, \mathbf{v}) - \sum_{k \in \Lambda_V} (A_k \mathbf{u}_k, \mathbf{v})_{\Omega_k}, \quad \forall \mathbf{v} \in V_h^0(\Omega_V^{half});$$

Step 4. With the trace $\Phi_h = \gamma(\sum_{V \in \mathcal{N}_d} \mathbf{u}_V)|_\Gamma$, compute the A -harmonic extension of Φ_h on each Ω_k to obtain $\mathbf{u}^\perp \in V_h^\perp(\Omega)$. This leads to

$$\mathbf{u} = \mathbf{u}_d + \sum_{k=1}^N \mathbf{u}_k + \mathbf{u}^\perp.$$

Remark 3.1. Notice that all the subproblems in **Algorithm 3.1** correspond to the same bilinear form as $\mathcal{A}(\cdot, \cdot)$ (but with different finite element spaces). We point out that each vertex-related space $V_h^0(\Omega_V^{half})$ has almost the same degrees of freedom with an original subdomain space $V_h^0(\Omega_k)$. Moreover, the local problem in Step 4 has the same stiffness matrix with that in Step 2 (with different right hands only). Thus the implementation of Step 4 is very cheap by using LU decomposition made in Step 2 for each local stiffness matrix (if Step 2 is implemented in the direct method). All this shows that **Algorithm 3.1** is easy and cheap to implement.

3.3. An approximation of the vertex-related solver B_V . In order to reduce the cost for the implementation of Step 3 in **Algorithm 3.1**, we would like to replace each space $V_h^0(\Omega_V^{half})$ by a smaller space. In Step 4 we need only to use the values of \mathbf{u}_V on Γ_V^{half} , so we only hope to get a rough approximation of $\mathbf{u}_V|_{\Gamma_V^{half}}$ but do not care for the accuracy of \mathbf{u}_V at the nodes in the interior of $\Omega_V^{half} \setminus \Gamma_V^{half}$. Intuitively, the accuracy of an approximation for \mathbf{u}_V mainly depends on the grids nearing Γ_V^{half} and is not sensitive to the grids far from Γ_V^{half} . Based on this observation, we can construct an auxiliary non-uniform partition $\tilde{\mathcal{T}}_h^V$ on Ω_V^{half} , for which the original fine grid on Γ_V^{half} are kept and the grid in the interior of $\Omega_V^{half} \setminus \Gamma_V^{half}$ gradually becomes coarser when nodes are far from Γ_V^{half} . The auxiliary partition

$\tilde{\mathcal{T}}_h^V$ can be easily generated by the existing software [25]. With this auxiliary partition $\tilde{\mathcal{T}}_h^V$, we can define a new linear finite element space $\tilde{V}_h^0(\Omega_V^{half})$, each function in which vanishes outside Ω_V^{half} . Now we replace the space $V_h^0(\Omega_V^{half})$ in Step 3 by $\tilde{V}_h^0(\Omega_V^{half})$ and we get a variant Step 3' of Step 3. The resulting solver, which is denoted by \tilde{B}_V , can be viewed as an approximation of B_V . Since the dimension of $\tilde{V}_h^0(\Omega_V^{half})$ is much smaller than that of $V_h^0(\Omega_V^{half})$, the implementation of Step 3' (i.e., the action of \tilde{B}_V^{-1}) is much cheaper than that of Step 3 (i.e., the action of B_V^{-1}). For convenience, we use \tilde{B} to denote the preconditioner defined by (3.3) with B_V being replaced by \tilde{B}_V .

3.4. An extension to the case with irregular subdomains. In this subsection, we consider the case that the subdomains $\{\Omega_k\}$ in the previous sections are irregular, i.e., some subdomains Ω_k are not polyhedrons with finite faces, see Figure 2. This situation appears when subdomains $\{\Omega_k\}$ are automatically generated by the software Metis [34] for given fine meshes.

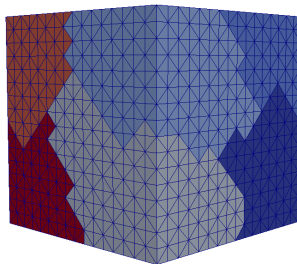


FIGURE 2. irregular partition for Ω

Notice that the subdomains generated by this software may be geometrically non-conform, i.e., the common part of two neighboring subdomains is not a complete face of one of the two subdomains. In this situation, the information on substructuring vertices, edges and faces are in general unknown and can not be directly obtained. This means that, before implementing the proposed preconditioner for this case, one needs to get information on coarse vertices (information on coarse edges and coarse faces is also needed for the BDDC method or the FETI-DP method). In order to extend the proposed preconditioner to the case with irregular subdomains, we recall a precise definition of substructuring vertices (refer to [41]) and give a variant of the coarse subspace $V_d(\Omega)$.

- Substructuring vertices

We first extend the definition in [41]. Let Γ denote the interface, which is the union of all the common parts of two neighboring subdomains, and let \mathcal{N}_Γ denote

the set of nodes on Γ . We need to decompose the set \mathcal{N}_Γ into the union of disjoint equivalence classes $\{\mathcal{N}_l\}$. For this purpose, we define an index set of subdomains for each $p \in \mathcal{N}_\Gamma$ by

$$\Lambda(p) = \{k : p \in \partial\Omega_k\}.$$

Two nodes $p, q \in \mathcal{N}_\Gamma$ belong to a same equivalence class \mathcal{N}_l if and only if $\Lambda(p) = \Lambda(q)$. For example, all the nodes on the common part of two neighboring subdomains constitute a class \mathcal{N}_l . In particular, some class \mathcal{N}_l may contain only one node on Γ . For convenience, let \mathcal{N}_d^* denote the union of all the single point sets \mathcal{N}_l , each of which contains only one node in \mathcal{N}_Γ .

For the standard domain decomposition with polyhedral subdomains, the set \mathcal{N}_d^* is just the subdomain vertex set used to define coarse subspace. However, the geometric structure of subdomains generated by Metis is very complicated, which makes \mathcal{N}_d^* contain too many vertices and some vertices in \mathcal{N}_d^* to be very close. In order to reduce the number of vertices and construct a practical coarse space that contains small degree of freedoms, we need to choose partial vertices from \mathcal{N}_d^* to get the desired vertex set $\mathcal{N}_d \subset \mathcal{N}_d^*$. The main idea is to remove the vertices that have very short distances from \mathcal{N}_d^* (here we omit the details).

- Coarse subspace

With the vertex set \mathcal{N}_d defined above, we can construct a coarse subspace as in [4] and [7]. Let \mathcal{T}_d denote the auxiliary coarse mesh generated by the vertex set \mathcal{N}_d , and let $\hat{V}_d(\Omega)$ denote the finite element space induced by \mathcal{T}_d . For the case with irregular subdomains, the space $\hat{V}_d(\Omega)$ is not a subspace of $V_h(\Omega)$ yet, except for some very particular examples. Let $\Pi_h : \hat{V}_d(\Omega) \rightarrow V_h(\Omega)$ be the standard interpolation operator. Then the coarse space $V_d(\Omega) \subset V_h(\Omega)$ can be defined by:

$$V_d(\Omega) = \left\{ \Pi_h \mathbf{v} : \mathbf{v} \in \hat{V}_d(\Omega) \right\}. \quad (3.4)$$

The numerical results in section 5 will show that this coarse space is practical for elliptic-type problems in the irregular partition situation.

- Vertex-related subdomains

For each vertex $v \in \mathcal{N}_d$, we consider all the subdomains that contain v as their common vertex. Let Ξ_v denote the set of all the vertices of these subdomains except v itself. We use the software in Tetgen [45] to generate a polyhedron $\hat{\Omega}_v$, which is the convex hull of the vertexes in Ξ_v . The vertex v can be regarded as the ‘‘center’’ of the polyhedron $\hat{\Omega}_v$. Then we shrink this polyhedron to new one $\hat{\Omega}_v^{half}$ with half size of $\hat{\Omega}_v$, but keep the ‘‘center’’ v . Now we define the v -related subdomain Ω_v^{half} as the union of all the fine elements whose vertexes are contained in the contracted polyhedron $\hat{\Omega}_v^{half}$. Here some auxiliary vertex subdomains Ω_v^{half} perhaps need to be extended with several fine element layers such that the union of all the local interfaces $\Omega_v^{half} \cap \Gamma$ form an open covering of Γ .

3.5. Comparisons between the proposed method and some existing methods. In this subsection, we further investigate the proposed preconditioner B and compare it with some existing preconditioners

- On the coarse solver

According to the explanations in Introduction, the coarse solver A_d described in Subsection 3.2 is the simplest and almost the cheapest one in the existing non-overlapping DDMs for three-dimensional problems (see Introduction for the details). More importantly, the construction of A_d is unified and does not depend on the considered models.

- On the interface solvers

When the proposed coarse solver A_d is used, cheap “edge” solvers (and “face” solvers) need to be designed. Comparing [30] with [29] (see also [15] and [53]), we know that the constructions of the existing “edge” solvers are based on estimates of the norms induced from the interface operators restricted on the edges and so depend on the considered models. In the proposed preconditioner B , the construction of the vertex-related solvers B_V (which play the role of interface solver) is unified and independent of the bilinear $\mathcal{A}(\cdot, \cdot)$.

Constructing interface solver by overlapping domain decomposition was also considered in the vertex space method (see [46]) and the interface overlapping additive Schwarz method (see Subsection 7.2 of [53]). But the spaces $V_h^\perp(\Omega_V^{half})$ introduced in Subsection 3.2 have essential difference from the local interface spaces proposed in [46]) and [53], where exact harmonic extensions in all Ω_k were required (moreover, large overlap was emphasized in [53]). Thanks to this difference, we can define the cheaper (inexact) local interface solvers B_V .

- Comparisons with the BDDC method

Undoubtedly, the BDDC method is one of the most interesting non-overlapping domain decomposition methods. The BDDC method was first introduced in [11], and then was studied and developed in many papers, see, for example, [13]-[14], [38]-[39], [41]-[42] and [51]. The main idea of the BDDC method is to build a coarse component by the weighted sum of functions that minimize discrete local energies subject to certain primal constraints across the subdomain interface. How to choose suitable constraints, which heavily depends on the considered models, is the key technique in the BDDC method, as in FETI-DP method. The BDDC algorithms solve linear systems of primal unknowns, in contrast to FETI-DP algorithms.

Although the proposed method and the BDDC method were designed based on different ideas, they possess the following common merits: (1) the coarse matrix has a favorable sparsity pattern since two coarse dofs are coupled in the coarse stiffness matrix only if both dofs appear together in at least one substructure; (2) all the subproblems to be solved preserve the positive definiteness of the original problem; (3) the coarse stiffness matrix can be preconditioned more easily since it

has almost the same structure as the original stiffness matrix. The proposed method and the BDDC method have two respective advantages: for the proposed method, the designs of the coarse solver and local solvers are unified and do not depend on the considered model, and the basis functions in the coarse space can be directly obtained, without solving minimization problems; for the BDDC method, no coarse mesh is involved so it is particularly attractive if any coarse mesh cannot directly generate a subspace of the solution, also the BDDC preconditioner in general has very fast convergence.

4. ANALYSIS ON THE CONVERGENCE OF THE PRECONDITIONER

4.1. A general result. It is known that, when the simplest coarse solver A_d is used to the construction of substructuring preconditioners, the condition number of the resulting preconditioned system is not nearly optimal except for some particular cases (the coefficients in the considered equation have no large jump or the subdomains have no internal cross-point). Fortunately, this unsatisfactory condition number has no large influence on the convergence rate of the PCG iteration for solving the underlying system, provided that the number of the “bad” eigenvalues of the preconditioned system is small (refer to [52]).

Let $\tilde{V}_h(\Omega)$ be a subspace of $V_h(\Omega)$, and let $m_0 = \dim(V_h(\Omega)) - \dim(\tilde{V}_h(\Omega))$. Assume that the number m_0 is small and is independent of the mesh size h and the subdomain size d . We use $\lambda_{m_0+1}(B^{-1}A)$ to denote the minimal eigenvalue of the restriction of $B^{-1}A$ on the subspace $\tilde{V}_h(\Omega)$, and define $\kappa_{m_0+1}(B^{-1}A)$ as the *reduced condition number* of $B^{-1}A$ associated with the subspace $\tilde{V}_h(\Omega)$. Namely,

$$\kappa_{m_0+1}(B^{-1}A) = \frac{\lambda_{\max}(B^{-1}A)}{\lambda_{m_0+1}(B^{-1}A)}.$$

Then the convergence rate of the PCG method with the preconditioner B for solving the system (2.3) is determined by the *reduced condition number* $\kappa_{m_0+1}(B^{-1}A)$ (see [52] for the details). In this subsection, we give a general result for the estimate of $\kappa_{m_0+1}(B^{-1}A)$.

For ease of notation, the symbols \lesssim , \gtrsim and $\bar{\approx}$ will be used in the rest of this paper. That $x_1 \lesssim y_1$, $x_2 \gtrsim y_2$ and $x_3 \bar{\approx} y_3$, mean that $x_1 \leq C_1 y_1$, $x_2 \geq c_2 y_2$ and $c_3 x_3 \leq y_3 \leq C_3 x_3$ for some constants C_1 , c_2 , c_3 and C_3 that are independent of h and d .

Let $I_h^V : V_h(\Omega) \rightarrow V_h^0(\Omega_V^{half})$ denote a local “interpolation-type” operator such that, for any $\mathbf{w}_h \in V_h(\Omega)$, the unit decomposition condition holds, i.e., $\sum_V I_h^V \mathbf{w}_h \equiv \mathbf{w}_h$ on Ω .

We define the “extension-type” operator $E_V^\perp : V_h^0(\Gamma_V^{half}) \rightarrow V_h^\perp(\Omega_V^{half})$ such that, for any $\mathbf{w}_h \in V_h^0(\Omega_V)$, the function $E_V^\perp \mathbf{w}_h$ possesses the same degrees of freedom as \mathbf{w}_h in Γ_V^{half} . By the definition of $V_h^\perp(\Omega_V^{half})$, the function $E_V^\perp \mathbf{w}_h$ vanishes in the exterior of Ω_V^{half} and is discrete \mathcal{A} -harmonic in $\Omega_{V,k}^{half}$ for each $k \in \Lambda_V$.

In the rest of this paper, let $\|\cdot\|_A$ denote the norm induced by the inner-product $\mathcal{A}(\cdot, \cdot)$.

Theorem 4.1. *Assume that there exists an operator $\Pi_d : V_h(\Omega) \rightarrow V_d(\Omega)$ such that*

$$\|\Pi_d \mathbf{v}_h\|_A^2 \leq C(h, d) \|\mathbf{v}_h\|_A^2 \quad (4.5)$$

and

$$\sum_V \|E_V^\perp(I_h^V(\mathbf{v}_h - \Pi_d \mathbf{v}_h))\|_A^2 \leq C(h, d) \|\mathbf{v}_h\|_A^2 \quad (4.6)$$

for any $\mathbf{v}_h \in \tilde{V}_h(\Omega)$. Here the positive number $C(h, d)$ may weakly depends on h and d . Then we have $\kappa_{m_0+1}(B^{-1}A) \lesssim C(h, d)$.

Proof. Notice that the bilinear form $\mathcal{A}(\cdot, \cdot)$ possesses the local property, i.e., when $\mathbf{v}, \mathbf{w} \in V_h(\Omega)$ have disjoint support sets, we have $\mathcal{A}(\mathbf{v}, \mathbf{w}) = 0$. Then we can prove $\lambda_{\max}(B^{-1}A) \lesssim 1$ in the standard manner. It suffices to estimate $\lambda_{m_0+1}(B^{-1}A)$.

For any $\mathbf{v}_h \in \tilde{V}_h(\Omega)$, define $\mathbf{v}_d \in V_d(\Omega)$ as $\mathbf{v}_d = \Pi_d \mathbf{v}_h$ and set $\tilde{\mathbf{v}}_h = \mathbf{v}_h - \mathbf{v}_d$. With this $\tilde{\mathbf{v}}_h$, we define the function $\tilde{\mathbf{v}}_V \in V_h^0(\Omega_V)$ such that $\tilde{\mathbf{v}}_V = I_h^V \tilde{\mathbf{v}}_h$ on Γ_V^{half} and $\tilde{\mathbf{v}}_V$ is discrete \mathcal{A} -harmonic in each subdomain Ω_k . Then $\tilde{\mathbf{v}}_V \in V_h^\perp(\Omega_V)$. Define

$$\tilde{\mathbf{v}}_k^0 = (\tilde{\mathbf{v}}_h - \sum_{V \in \mathcal{N}_d} \tilde{\mathbf{v}}_V)|_{\Omega_k}. \quad (4.7)$$

Since the operators I_h^V satisfy the unit decomposition condition, we have $\tilde{\mathbf{v}}_k^0 \in V_h^0(\Omega_k)$. It follows by (4.7) that

$$\sum_{k=1}^N \tilde{\mathbf{v}}_k^0 = \tilde{\mathbf{v}}_h - \sum_{V \in \mathcal{N}_d} \tilde{\mathbf{v}}_V. \quad (4.8)$$

Then we build the decomposition

$$\mathbf{v}_h = \mathbf{v}_d + \sum_{k=1}^N \tilde{\mathbf{v}}_k^0 + \sum_{V \in \mathcal{N}_d} \tilde{\mathbf{v}}_V. \quad (4.9)$$

We need only to verify the stability of the decomposition.

By the definition of B_V , we have

$$(B_V \tilde{\mathbf{v}}_V, \tilde{\mathbf{v}}_V) = \|E_V^\perp(I_h^V \tilde{\mathbf{v}}_h)\|_A^2.$$

This, together with the assumption (4.6), leads to

$$\sum_V (B_V \tilde{\mathbf{v}}_V, \tilde{\mathbf{v}}_V) \leq C(h, d) \|\mathbf{v}_h\|_A^2. \quad (4.10)$$

Finally, using (4.9), together with (4.5) and (4.10), yields

$$\begin{aligned} & (A_d \mathbf{v}_d, \mathbf{v}_d) + \sum_{k=1}^N (A_k \tilde{\mathbf{v}}_k^0, \tilde{\mathbf{v}}_k^0) + \sum_{V \in \mathcal{N}_d} (B_V \tilde{\mathbf{v}}_V, \tilde{\mathbf{v}}_V) \\ & \lesssim C(h, d) \|\mathbf{v}_h\|_A^2, \quad \forall \mathbf{v}_h \in \tilde{V}_h(\Omega), \end{aligned} \quad (4.11)$$

which implies that

$$\lambda_{m_0+1}(B^{-1}A) \geq 1/C(h, d).$$

Now the desired result can be obtained directly. \square

4.2. Result for linear elasticity problems. In this subsection, we try to estimate the positive $C(h, d)$ in Theorem 4.1 for linear elasticity problems. As to Maxwell's equations, the proof is very complicated, which beyond the goal of this article.

Let's consider the linear elasticity problem:

$$\begin{cases} -\sum_{j=1}^3 \frac{\partial \sigma_{ij}}{\partial x_j}(\mathbf{u}) = f_i, & \text{in } \Omega \\ \mathbf{u} = 0, & \text{on } \partial\Omega \end{cases} \quad (4.12)$$

where $\mathbf{f} = (f_1 \ f_2 \ f_3)^T$ is an internal volume force, e.g. gravity (cf. [9]). The linearized strain tensor is defined by

$$\varepsilon = \varepsilon(\mathbf{u}) = [\varepsilon_{ij} = \frac{1}{2}(\frac{\partial u_i}{\partial x_j} + \frac{\partial u_j}{\partial x_i})],$$

and

$$\sigma_{ij}(\mathbf{u}) := \lambda \delta_{ij} \operatorname{div} \mathbf{u} + 2\mu \varepsilon_{ij}.$$

where λ and μ are the *Lamé* parameters (cf. [49]), which are positive functions.

The subspace $H_0^1(\Omega) \subset H^1(\Omega)$ is the set of functions having the zero trace on $\partial\Omega$. We introduce the vector value Sobolev space $(H_0^1(\Omega))^3$. Concerning the variational problem (2.1), we have $V(\Omega) := [H_0^1(\Omega)]^3$ and

$$\begin{aligned} \mathcal{A}(\mathbf{u}, \mathbf{v}) &= \int_{\Omega} (2\mu \varepsilon(\mathbf{u}) : \varepsilon(\mathbf{v}) + \lambda \operatorname{div} \mathbf{u} \cdot \operatorname{div} \mathbf{v}) d\mathbf{x}, \\ \langle \mathbf{F}, \mathbf{v} \rangle &= \int_{\Omega} \mathbf{f} \cdot \mathbf{v} d\mathbf{x} \end{aligned}$$

where

$$\varepsilon(\mathbf{u}) : \varepsilon(\mathbf{v}) := \sum_{i,j=1}^n \varepsilon_{ij}(\mathbf{u}) \varepsilon_{ij}(\mathbf{v}).$$

Let $R(K)$ be a subset of all linear polynomials on the element K of the form:

$$R(K) = \left\{ \mathbf{A} \cdot \mathbf{x} + \mathbf{C}; \mathbf{A} \in \mathbb{R}^{3 \times 3}, \mathbf{C} \in \mathbb{R}^3, \mathbf{x} \in K \right\}.$$

To our knowledge, there seems no work to analyze nearly optimal substructuring preconditioners for three-dimensional problems with irregular subdomains, which bring particular difficulties. Thus, here we only consider the case with regular subdomains. Assume that Ω can be written as the union of polyhedral subdomains D_1, \dots, D_{N_0} , such that $\lambda(\mathbf{x}) = \lambda_r$ and $\mu(\mathbf{x}) = \mu_r$ for $x \in D_r$, with every λ_r and μ_r being a positive constant. In applications, N_0 is a *fixed* positive integer, so the diameter of each D_r is $O(1)$. For the analysis, we assume that every subdomain Ω_k

is a polyhedron. It is certain that the subdomains Ω_k should satisfy the condition: each D_r is the union of some subdomains in $\{\Omega_k\}$.

The null space $\ker(\varepsilon)$ is the space of rigid body motions. In three dimensions, the corresponding space is spanned by three translations

$$\mathbf{r}_1 := \begin{bmatrix} 1 \\ 0 \\ 0 \end{bmatrix}, \quad \mathbf{r}_2 := \begin{bmatrix} 0 \\ 1 \\ 0 \end{bmatrix}, \quad \mathbf{r}_3 := \begin{bmatrix} 0 \\ 0 \\ 1 \end{bmatrix},$$

and three rotation

$$\mathbf{r}_4 := \begin{bmatrix} 0 \\ x_3 \\ -x_2 \end{bmatrix}, \quad \mathbf{r}_5 := \begin{bmatrix} -x_3 \\ 0 \\ x_1 \end{bmatrix}, \quad \mathbf{r}_6 := \begin{bmatrix} -x_2 \\ x_1 \\ 0 \end{bmatrix}.$$

Let $\Lambda = \{k : \partial D_k \cap \partial \Omega = \emptyset\}$ denote the index set of the subdomains D_1, \dots, D_{N_0} that do not touch the boundary of Ω , and set

$$\tilde{V}_h(\Omega) = \{\mathbf{v}_h \in V_h(\Omega) : \sum_{i=1}^6 \left| \int_{D_k} \mathbf{r}_i \cdot \mathbf{v}_h d\mathbf{x} \right| = 0, k \in \Lambda\}.$$

Let n_0 denote the number of the subdomains that do not touch $\partial \Omega$, i.e., $n_0 = \dim(\Lambda)$, and set $m_0 = 6n_0$.

Theorem 4.2. *For the linear elasticity problems described above, we have*

$$\kappa_{m_0+1}(B^{-1}A) \lesssim \log(1/d) \log^2(d/h). \quad (4.13)$$

When the coefficients $\mu(x)$ and $\lambda(x)$ have no large jump across the interface Γ , or there is no cross-point in the distribution of the jumps of the coefficients, the factor $\log(1/d)$ in the above inequalities can be removed.

In order to prove this result, we need several auxiliary results. In the following we use $D \subset \Omega$ to denote a generic polyhedron in D_1, \dots, D_{N_0} . It is clear that

$$\|\varepsilon(\mathbf{v})\|_{0,D} \leq \|\nabla \mathbf{v}\|_{0,D} \quad \text{and} \quad \|\operatorname{div}(\mathbf{v})\|_{0,D} \leq \|\nabla \mathbf{v}\|_{0,D}, \forall \mathbf{v} \in [H^1(D)]^3. \quad (4.14)$$

The following lemma can be obtained by Korn inequality and the result in [35] and [44].

Lemma 4.1. *There exist positive constants c_0 and C_0 , such that*

$$c_0 \|\nabla \mathbf{v}\|_{0,D} \leq \|\varepsilon(\mathbf{v})\|_{0,D} \leq C_0 \|\nabla \mathbf{v}\|_{0,D}$$

for any function $\mathbf{v} \in [H^1(D)]^3$, which satisfies either $(\mathbf{v}, \mathbf{r})_{L_2(D)} = 0$ for each $\mathbf{r} \in \ker(\varepsilon)$ or \mathbf{v} vanishes on a face of D .

□

Define the weighted norm

$$\|\mathbf{v}\|_{1,\Omega_k} = (|\mathbf{v}|_{1,\Omega_k}^2 + d^{-2} \|\mathbf{v}\|_{0,\Omega_k}^2)^{1/2}$$

We assume that there exists constant c_0, C_0 , such that

$$c_0\lambda_r \leq \mu_r \leq C_0\lambda_r, \quad \forall D_r \subset \Omega, \quad r = 1, \dots, D_{N_0}.$$

Define the weighted L^2 -inner product and the weighted H^1 -inner product as follows:

$$(\mathbf{u}, \mathbf{v})_{L_\lambda^2(\Omega)} = \sum_{r=1}^{N_0} \lambda_r \int_{D_r} \mathbf{u} \cdot \mathbf{v} d\mathbf{x}, \quad \mathbf{u}, \mathbf{v} \in [L^2(\Omega)]^3.$$

$$(\mathbf{u}, \mathbf{v})_{H_\lambda^1(\Omega)} = \sum_{r=1}^{N_0} \lambda_r \int_{D_r} \nabla \mathbf{u} \cdot \nabla \mathbf{v} d\mathbf{x}, \quad \mathbf{u}, \mathbf{v} \in [H_0^1(\Omega)]^3.$$

Let $\|\cdot\|_{L_\lambda^2(\Omega)}$ and $|\cdot|_{H_\lambda^1(\Omega)}$ denote, respectively, the norm and the semi-norm induced by the inner product $(\cdot, \cdot)_{L_\lambda^2(\Omega)}$ and $(\cdot, \cdot)_{H_\lambda^1(\Omega)}$. For convenience, define

$$\|\mathbf{v}\|_{H_\lambda^1(\Omega)} = (|\mathbf{v}|_{H_\lambda^1(\Omega)}^2 + d^{-2}\|\mathbf{v}\|_{L_\lambda^2(\Omega)}^2)^{1/2}$$

Let $Q_d^\lambda : [L^2(\Omega)]^3 \rightarrow V_d(\Omega)$ be the weighted L^2 projections defined by

$$(Q_d^\lambda \mathbf{v}, \mathbf{w})_{L_\lambda^2(\Omega)} = (\mathbf{v}, \mathbf{w})_{L_\lambda^2(\Omega)}, \quad \forall \mathbf{v} \in [L^2(\Omega)]^3, \mathbf{w} \in V_d(\Omega). \quad (4.15)$$

It is clear that

$$\tilde{V}_h(\Omega) \subset \{\mathbf{v}_h \in V_h(\Omega) : \int_{D_k} \mathbf{v}_h d\mathbf{x} = \mathbf{0}, \quad k \in \Lambda\}.$$

Then, by the result given in [52], we have

Lemma 4.2. *The weighted L^2 projection Q_d^λ satisfies*

$$\|(Q_d^\lambda - I)\mathbf{v}\|_{L_\lambda^2(\Omega)}^2 \lesssim d^2 \log(1/d) |\mathbf{v}|_{H_\lambda^1(\Omega)}^2, \quad \forall \mathbf{v} \in \tilde{V}_h(\Omega) \quad (4.16)$$

and

$$|Q_d^\lambda \mathbf{v}|_{H_\lambda^1(\Omega)}^2 \lesssim \log(1/d) |\mathbf{v}|_{H_\lambda^1(\Omega)}^2, \quad \forall \mathbf{v} \in \tilde{V}_h(\Omega). \quad (4.17)$$

□

Remark 4.1. *When the coefficient $\lambda(\mathbf{x})$ has no jump across the interface Γ , or there is no cross-point in the distribution of the jumps of the coefficient, the factor $\log(1/d)$ in the inequalities (4.16) and (4.17) can be removed.*

The following lemma is a direct consequence of Lemma 4.1 and (4.14).

Lemma 4.3. *The following norm equivalence holds*

$$\|\mathbf{v}\|_A^2 \approx |\mathbf{v}|_{H_\lambda^1(\Omega)}^2, \quad \forall \mathbf{v} \in \tilde{V}_h(\Omega). \quad (4.18)$$

□

Next we present a stability result of discrete harmonic functions in some $\Omega_{\mathbf{v},k}^{half}$. In order to simplify the analysis, we assume that all our subdomains Ω_k are cubes and we only consider a specific way for the construction of $\Omega_{\mathbf{v}}^{half}$.

For each $\mathbf{v} \in \mathcal{N}_d$, we choose an auxiliary cube $G_{\mathbf{v}}$ with the size d and the center \mathbf{v} . Define $\Omega_{\mathbf{v}}^{half}$ as the union of all the elements, each of which has at least one

vertex located in the cube or just touching the boundary of this cube. Notice that G_V may be slightly smaller than Ω_V^{half} (we consider only the case with small overlap). In this case, the size of $\Omega_{V,k}^{half}$ is $d/2$ for each $k \in \Lambda_V$. Notice that $\Omega_{V,k}^{half}$ is not a polyhedron, i.e., it has a quite irregular boundary, so the desired stability result can not be proved in the standard way. It is easy to see that $\Omega_{V,k}^{half}$ is a Jones domain, whose definition and properties can be found in [33] and [37]. Intuitively, a Jones domain means that it satisfies twisted cone condition and can't be too oblate relative to its diameter.

Let \mathcal{E}_{ij} be the common face between two neighboring subdomains O_i and O_j . Define

$$V_h^{ij}(O_k) = \{v_h \in V_h(O_k) : v_h(\mathbf{x}) = 0 \text{ at all nodes of } \partial O_k \setminus \mathcal{E}_{ij}\} \quad (k = i, j).$$

Before giving the stability result, we recall an ‘‘interface’’ extension lemma proved in [37].

Lemma 4.4. [37] *Assume that O_i is a domain with a complement which is a Jones domain. Then, there exists an extension operator*

$$E_{ji}^h : V_h^{ij}(O_j) \rightarrow V_h^{ij}(O_i)$$

such that

$$(E_{ji}^h v_h)|_{\Gamma_{ij}} = v_h|_{\Gamma_{ij}} \quad \text{and} \quad |E_{ji}^h v_h|_{H^1(O_i)} \lesssim |v_h|_{H^1(O_j)}, \quad \forall v_h \in V_h^{ij}(O_j).$$

□

To distinguish with the elastic harmonic extension, we define the discrete harmonic space associated with Laplace-type operator

$$V_h^H(\Omega) = \{\mathbf{v} \in V_h(\Omega) : (\nabla \mathbf{v}, \nabla \mathbf{w}) = 0, \forall \mathbf{w} \in V_h^0(\Omega_k), k = 1 \cdots N\}.$$

For each $\mathbf{v} \in \mathcal{N}_d$, define the vertex-related local harmonic spaces

$$V_h^H(\Omega_V) = \{\mathbf{v} \in V_h^H(\Omega) : \text{the trace of } \mathbf{v} \text{ belongs to } V_h^0(\Gamma_V^{half})\} \subset V_h^0(\Omega_V)$$

and

$$V_h^H(\Omega_V^{half}) = \{\mathbf{v} \in V_h^0(\Omega_V^{half}) : (\nabla \mathbf{v}, \nabla \mathbf{w}) = 0, \forall \mathbf{w} \in V_h^0(\Omega_{V,k}^{half}) \text{ with } k \in \Lambda_V\}.$$

Lemma 4.5. *Let $\mathbf{u}_V^{half} \in V_h^H(\Omega_V^{half})$ and $\mathbf{u}_V \in V_h^H(\Omega_V)$. Assume that the two functions satisfy $\mathbf{u}_V = \mathbf{u}_V^{half}$ on Γ_V^{half} . Then we have*

$$|\mathbf{u}_V^{half}|_{H_\lambda^1(\Omega)} \lesssim |\mathbf{u}_V|_{H_\lambda^1(\Omega)}. \quad (4.19)$$

Proof. For $k \in \Lambda_V$, we define $\mathbf{u}_{V,k}^{half} = \mathbf{u}_V^{half}|_{\Omega_k}$ and $\mathbf{u}_{V,k} = \mathbf{u}_V|_{\Omega_k}$. It suffices to prove that

$$|\mathbf{u}_{V,k}^{half}|_{1,\Omega_k} \lesssim |\mathbf{u}_{V,k}|_{1,\Omega_k}, \quad \forall k \in \Lambda_V. \quad (4.20)$$

By the triangle inequality, we have

$$|\mathbf{u}_{V,k}^{half}|_{1,\Omega_k} \leq |\mathbf{u}_{V,k}|_{1,\Omega_k} + |\mathbf{u}_{V,k}^{half} - \mathbf{u}_{V,k}|_{1,\Omega_k}. \quad (4.21)$$

Set $\Omega_{V,k}^\partial = \Omega_k \setminus \Omega_{V,k}^{half}$ and let $F_{V,k}$ denote the common interface of $\Omega_{V,k}^\partial$ and $\Omega_{V,k}^{half}$. Since $\mathbf{u}_{V,k}^{half}$ vanishes on $F_{V,k}$, it can be naturally extended into $\Omega_{V,k}^\partial$ by zero. Let $\tilde{\mathbf{u}}_{V,k}^{half} \in V_h(\Omega_k)$ denote the resulting extension, and define $\mathbf{u}_{V,k}^\partial = \mathbf{u}_{V,k} - \tilde{\mathbf{u}}_{V,k}^{half}$. Then $\mathbf{u}_{V,k}^\partial|_{\Omega_{V,k}^\partial} = \mathbf{u}_{V,k}$ and $\mathbf{u}_{V,k}^\partial$ vanishes on $\partial\Omega_{V,k}^\partial \setminus F_{k,V}$. Using Lemma 4.4, there exists an extension $\tilde{\mathbf{u}}_{V,k}^\partial$ of $\mathbf{u}_{V,k}^\partial$ such that $\tilde{\mathbf{u}}_{V,k}^\partial \in V_h(\Omega_{V,k}^{half})$ and $\tilde{\mathbf{u}}_{V,k}^\partial = \mathbf{u}_{V,k}^\partial$ on $F_{V,k}$. Moreover, the extension $\tilde{\mathbf{u}}_{V,k}^\partial$ satisfies

$$|\tilde{\mathbf{u}}_{V,k}^\partial|_{1,\Omega_{V,k}^{half}} \lesssim |\mathbf{u}_{V,k}^\partial|_{1,\Omega_{V,k}^\partial} \quad \text{and} \quad \tilde{\mathbf{u}}_{V,k}^\partial = \mathbf{u}_{V,k}^\partial \text{ on } \partial\Omega_{V,k}^{half}. \quad (4.22)$$

Notice that $\mathbf{u}_{V,k}^\partial$ is Laplace-type discrete harmonic in the interior of $\Omega_{V,k}^{half}$, by (4.22) we obtain

$$|\mathbf{u}_{V,k}^\partial|_{1,\Omega_{V,k}^{half}} \leq |\tilde{\mathbf{u}}_{V,k}^\partial|_{1,\Omega_{V,k}^{half}} \lesssim |\mathbf{u}_{V,k}^\partial|_{1,\Omega_{V,k}^\partial} = |\mathbf{u}_{V,k}|_{1,\Omega_{V,k}^\partial}. \quad (4.23)$$

Combing this with (4.21) leads to (4.20). Then (4.19) follows by (4.20). \square

Lemma 4.6. *Let $\mathbf{u}^\perp \in V_h^\perp(\Omega_V)$, $\mathbf{u}^H \in V_h^H(\Omega_V)$ and $\mathbf{u}^\perp = \mathbf{u}^H$ on Γ_V^{half} . Then we have*

$$(B_V \mathbf{u}^\perp, \mathbf{u}^\perp) \lesssim |\mathbf{u}^H|_{H_\lambda^1} \quad (4.24)$$

Proof. Define $\mathbf{u}^{half} \in V^\perp(\Omega_V^{half})$ such that $\mathbf{u}^{half} = \mathbf{u}^\perp$ on Γ_V^{half} . According to the definition of B_V , we know that

$$(B_V \mathbf{u}^\perp, \mathbf{u}^\perp) = \|\mathbf{u}^{half}\|_A^2. \quad (4.25)$$

Let $\tilde{\mathbf{u}}^{half} \in V^H(\Omega_V^{half})$ and satisfy $\tilde{\mathbf{u}}^{half} = \mathbf{u}^{half}$ on Γ_V^{half} . For each $k \in \Lambda_V$, the function \mathbf{u}^{half} is elastic-type discrete harmonic and $\tilde{\mathbf{u}}^{half}$ is Laplace-type discrete harmonic in the interior of $\Omega_{V,k}^{half}$. Then, by (4.14), we have

$$\|\mathbf{u}^{half}\|_A^2 \lesssim |\tilde{\mathbf{u}}^{half}|_{H_\lambda^1(\Omega)}^2. \quad (4.26)$$

Using Lemma 4.5, we know that

$$|\tilde{\mathbf{u}}^{half}|_{H_\lambda^1(\Omega)}^2 \lesssim |\mathbf{u}^H|_{H_\lambda^1(\Omega)}^2. \quad (4.27)$$

Then (4.24) follows by (4.25), (4.26) and (4.27). \square

For a vector-valued function $\mathbf{v} = (v_1 \ v_2 \ v_3)^T \in (H^1(\Omega_k))^3$, we define the $H^{1/2}$ -norm

$$\|\mathbf{v}\|_{1/2,\partial\Omega_k} = (|\mathbf{v}|_{1/2,\partial\Omega_k}^2 + d^{-1}\|\mathbf{v}\|_{0,\partial\Omega_k}^2)^{1/2} \quad \text{with} \quad |\mathbf{v}|_{1/2,\partial\Omega_k}^2 = \sum_{i=1}^3 |v_i|_{1/2,\partial\Omega_k}^2.$$

For a face F of $\partial\Omega_k$ and $\mathbf{v}_h \in V_h^0(F)$, let $\tilde{\mathbf{v}}_h \in V_h(\partial\Omega_k)$ denotes the zero extension of \mathbf{v}_h . Define the norm

$$\|\mathbf{v}_h\|_{H_{00}^{1/2}(F)}^2 = |\tilde{\mathbf{v}}_h|_{1/2,\partial\Omega_k}^2.$$

For a given subset $K \subset \Omega$, define a restriction operator $I_K^0 : V_h(\Omega) \rightarrow V_h^0(K)$ as follows: $(I_K^0 \mathbf{v})(x) = \mathbf{v}(x)$ for any $x \in K \cap \mathcal{N}_h$ and $(I_K^0 \mathbf{v})(x) = \mathbf{0}$ for $x \in \Omega \setminus K$. Similarly, we can define $I_K^0 : V_h(\Gamma) \rightarrow V_h^0(K)$ for a subset K of the interface Γ .

Let v be a given vertex. For a face F that has v as one of its vertices, let F_V^{in} denote the intersection of F and Γ_V^{half} . In the following we prove an extension result on the norm $H_{00}^{1/2}(F_V^{in})$.

For convenience, we show F and F_V^{in} in Fig. 3, where the big square $ABCV$ denotes F . Let l_0 , l_1 , l_2 denote the broken segments QH (the blue curve), DE (the yellow curve) and ET (the red curve), respectively. Then F_V^{in} is just the area surrounded by l_1 , l_2 , the straight segments \overline{DV} and \overline{TV} . In Fig. 3, the smaller square $HNMV$ denotes the intersection of F with the auxiliary cube G_V described behind Lemma 4.3. For the proof, we define an auxiliary square $SVIJ$ (which is denoted by F_V^{aux}) such that the distance between \overline{MN} and \overline{SJ} is approximately equal to $h/2$.

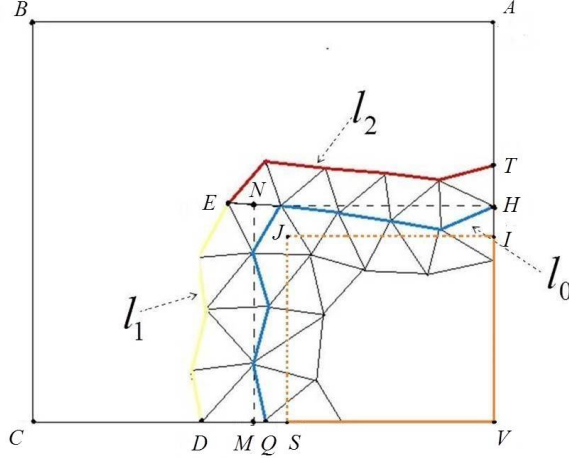


FIGURE 3. the relation between F and F_V^{in}

Lemma 4.7. *For a subdomain Ω_k , let $F_V^{in} \subset \partial\Omega_k$ be defined above. Then we have the face inequality*

$$\|I_{F_V^{in}}^0 \mathbf{v}_h\|_{H_{00}^{1/2}(F_V^{in})} \lesssim \log(d/h) \|\mathbf{v}_h\|_{1, \Omega_k}, \quad \forall \mathbf{v}_h \in V_h(\Omega_k). \quad (4.28)$$

Proof. As in Lemma 3.1 of [13], we can prove the “edge” inequality

$$\|\mathbf{v}_h\|_{0, l_i} \lesssim \log^{1/2}(d/h) \|\mathbf{v}_h\|_{1, \Omega_k}, \quad i = 0, 1, 2. \quad (4.29)$$

It is known that

$$\|I_{F_V^{in}}^0 \mathbf{v}_h\|_{H_{00}^{1/2}(F_V^{in})}^2 \approx \|I_{F_V^{in}}^0 \mathbf{v}_h\|_{1/2, F_V^{in}}^2 + \int_{F_V^{in}} \frac{|I_{F_V^{in}}^0 \mathbf{v}_h|^2}{\text{dist}(\mathbf{x}, \partial F_V^{in})} ds(\mathbf{x}). \quad (4.30)$$

It follows by (4.29) that

$$\begin{aligned}
|I_{\mathbb{F}_V^{in}}^0 \mathbf{v}_h|_{1/2, \mathbb{F}_V^{in}} &\lesssim |\mathbf{v}_h|_{1/2, \mathbb{F}_V^{in}} + \sum_{i=1}^2 \|\mathbf{v}_h\|_{0, l_i} + \|\mathbf{v}_h\|_{0, \overline{D\mathbb{V}}} + \|\mathbf{v}_h\|_{0, \overline{G\mathbb{V}}} \\
&\lesssim |\mathbf{v}_h|_{1/2, \partial\Omega_k} + \log^{1/2}(d/h) \|\mathbf{v}_h\|_{1, \Omega_k} \\
&\lesssim \log^{1/2}(d/h) \|\mathbf{v}_h\|_{1, \Omega_k}.
\end{aligned} \tag{4.31}$$

Let \mathbb{F}_V^{aux} denote the auxiliary square $SVIJ$ shown in FIG. 3. Then we have

$$\begin{aligned}
\int_{\mathbb{F}_V^{in}} \frac{|I_{\mathbb{F}_V^{in}}^0 \mathbf{v}_h(\mathbf{x})|^2}{\text{dist}(\mathbf{x}, \partial\mathbb{F}_V^{in})} ds(\mathbf{x}) &\equiv h^2 \sum_{p_i \in \mathcal{N}_h \cap \mathbb{F}_V^{in}} \frac{|\mathbf{v}_h(p_i)|^2}{\text{dist}(p_i, \partial\mathbb{F}_V^{in})} \\
&\lesssim h^2 \sum_{p_i \in \mathcal{N}_h \cap l_0} \frac{|\mathbf{v}_h(p_i)|^2}{\text{dist}(p_i, \partial\mathbb{F}_V^{in})} + h^2 \sum_{\substack{p_i \in \mathcal{N}_h \cap \mathbb{F}_V^{in} \\ p_i \notin l_0}} \frac{|\mathbf{v}_h(p_i)|^2}{\text{dist}(x_i, \partial\mathbb{F}_V^{in})} \\
&\lesssim \|\mathbf{v}_h\|_{0, l_0}^2 + \int_{\mathbb{F}_V^{aux}} \frac{|\mathbf{v}_h(\mathbf{x})|^2}{\text{dist}(\mathbf{x}, \partial\mathbb{F}_V^{in})} ds(\mathbf{x}).
\end{aligned} \tag{4.32}$$

As in Lemma 4.10 in [53], we can verify that

$$\int_{\mathbb{F}_V^{aux}} \frac{|\mathbf{v}_h(\mathbf{x})|^2}{\text{dist}(\mathbf{x}, \partial\mathbb{F}_V^{in})} ds(\mathbf{x}) \lesssim \log^2(d/h) \|\mathbf{v}_h\|_{1, \Omega_k}^2.$$

Substituting (4.29) and the above inequality into (4.32), yields

$$\int_{\mathbb{F}_V^{in}} \frac{|I_{\mathbb{F}_V^{in}}^0 \mathbf{v}_h(\mathbf{x})|^2}{\text{dist}(\mathbf{x}, \partial\mathbb{F}_V^{in})} ds(\mathbf{x}) \lesssim \log^2(d/h) \|\mathbf{v}_h\|_{1, \Omega_k}^2.$$

Plugging this and (4.31) in (4.30), leads to (4.28). \square

Proof of Theorem 4.2. It suffices to verify the assumptions given in Theorem 4.1. To this end, we choose the weighted L^2 projector Q_d^λ as the operator Π_d . Let $\tilde{\mathbf{v}}_h \in \tilde{V}_h(\Omega)$.

It follows by (4.14), (4.17) and (4.18) that

$$\|\Pi_d \mathbf{v}_h\|_A^2 \lesssim \log(1/d) \|\mathbf{v}_h\|_A^2. \tag{4.33}$$

Set $\tilde{\mathbf{v}}_h = \mathbf{v}_h - \Pi_d \mathbf{v}_h$. Using Lemma 4.2 and Lemma 4.3, yields

$$\|\tilde{\mathbf{v}}_h\|_{H_\lambda^1(\Omega)}^2 \lesssim \log(1/d) \|\mathbf{v}_h\|_A^2. \tag{4.34}$$

Let $I_h^V : V_h(\Omega) \rightarrow V_h^0(\Omega_V^{half})$ be the nodal weight interpolation: for $\mathbf{w}_h \in V_h(\Omega)$, the function $I_h^V \mathbf{w}_h$ vanishes outside Ω_V^{half} and $(I_h^V \mathbf{w}_h)(\mathbf{x}) = \frac{1}{q(\mathbf{x})} \mathbf{w}_h(\mathbf{x})$ for $\mathbf{x} \in \Omega_V^{half} \cap \mathcal{N}_h$, where $q(\mathbf{x})$ denotes the number of the subdomains Ω_V^{half} containing \mathbf{x} . Then all the operators I_h^V satisfy the unit decomposition condition described in the front of Theorem 4.1. Define $\tilde{\mathbf{v}}_V \in V_h^\perp(\Omega_V^{half})$ as $\tilde{\mathbf{v}}_V = E_V^\perp(I_h^V(\mathbf{v}_h - \Pi_d \mathbf{v}_h))$, where E_V^\perp is the extension operator defined in Subsection 4.1.

In the following, we estimate $\sum_V \|\tilde{\mathbf{v}}_V\|_A^2$.

For the function $\tilde{\mathbf{v}}_V \in V_h^\perp(\Omega_V^{half})$, define $\tilde{\mathbf{v}}_V^H \in V_h^H(\Omega_V)$ such that $\tilde{\mathbf{v}}_V^H = \tilde{\mathbf{v}}_V$ on Γ_V^{half} . It follows by Lemma 4.6 that

$$\begin{aligned} \|\tilde{\mathbf{v}}_V\|_A^2 &\lesssim |\tilde{\mathbf{v}}_V^H|_{H_\lambda^1(\Omega)}^2 = \sum_{k \in \Lambda_V} \lambda_k |\tilde{\mathbf{v}}_V^H|_{1, \Omega_k}^2 \\ &\lesssim \sum_{k \in \Lambda_V} \lambda_k |\tilde{\mathbf{v}}_V^H|_{1/2, \partial\Omega_k}^2. \end{aligned} \quad (4.35)$$

Thus we need only to estimate $|\tilde{\mathbf{v}}_V^H|_{1/2, \partial\Omega_k}^2$. It is clear that

$$\tilde{\mathbf{v}}_V^H|_{\partial\Omega_k} = I_V^0 \tilde{\mathbf{v}}_V^H + \sum_{\substack{E \in \mathcal{E}_V \\ E \subset \Gamma_k}} I_E^0 \tilde{\mathbf{v}}_V^H + \sum_{\substack{F \in \mathcal{F}_V \\ F \subset \Gamma_k}} I_F^0 \tilde{\mathbf{v}}_V^H. \quad (4.36)$$

Notice that $I_F^0 \tilde{\mathbf{v}}_V^H$ vanishes on $F \setminus F^{in}$. Then

$$\begin{aligned} \|I_F^0 \tilde{\mathbf{v}}_V^H\|_{H_{00}^{1/2}(F)}^2 &\lesssim \|I_{F^{in}}^0(I_h^V \tilde{\mathbf{v}}_h)\|_{H_{00}^{1/2}(F^{in})}^2 \\ &\lesssim \|I_{F^{in}}^0 \tilde{\mathbf{v}}_h\|_{H_{00}^{1/2}(F^{in})}^2 + \|I_{F^{in}}^0(\tilde{\mathbf{v}}_h - I_h^V \tilde{\mathbf{v}}_h)\|_{H_{00}^{1/2}(F^{in})}^2. \end{aligned} \quad (4.37)$$

By the construction of Ω_V^{half} (see the description behind Lemma 4.3), the overlap between intersecting faces F^{in} associated with two neighboring vertices contains at most two elements layer (refer to Fig. 3). Then, by the definitions of I_h^V and $I_{F^{in}}^0$, the function $I_{F^{in}}^0(\tilde{\mathbf{v}}_h - I_h^V \tilde{\mathbf{v}}_h)$ vanishes at all nodes except on l_0 shown in Fig. 3. In particular, when the overlap is just one element layer, we have $I_{F^{in}}^0(\tilde{\mathbf{v}}_h - I_h^V \tilde{\mathbf{v}}_h) \equiv 0$. By the inverse estimate and the discrete L^2 norms, we can deduce that

$$\|I_{F^{in}}^0(\tilde{\mathbf{v}}_h - I_h^V \tilde{\mathbf{v}}_h)\|_{H_{00}^{1/2}(F^{in})}^2 \lesssim \|(\tilde{\mathbf{v}}_h - I_h^V \tilde{\mathbf{v}}_h)\|_{0, l_0}^2 \lesssim \|\tilde{\mathbf{v}}_h\|_{0, l_0}^2.$$

Substituting this into (4.37), and using (4.28) and (4.29), yields

$$\|I_F^0 \tilde{\mathbf{v}}_V^H\|_{H_{00}^{1/2}(F)}^2 \lesssim \log^2(d/h) \|\tilde{\mathbf{v}}_h\|_{1, \Omega_k}^2. \quad (4.38)$$

In addition, using the vertex and edge lemmas in [53], we get

$$\|I_V^0 \tilde{\mathbf{v}}_V^H\|_{1/2, \partial\Omega_k} \lesssim \|I_V^0 \tilde{\mathbf{v}}_h\|_{1/2, \partial\Omega_k} \lesssim \log^{1/2}(d/h) \|\tilde{\mathbf{v}}_h\|_{1, \Omega_k}$$

and

$$\|I_E^0 \tilde{\mathbf{v}}_V^H\|_{1/2, \partial\Omega_k}^2 \lesssim \|I_E^0 \tilde{\mathbf{v}}_h\|_{1/2, \partial\Omega_k}^2 \lesssim \log^{1/2}(d/h) \|\tilde{\mathbf{v}}_h\|_{1, \Omega_k}.$$

By (4.36), together with (4.38) and the above two inequalities, gives

$$|\tilde{\mathbf{v}}_V^H|_{1/2, \partial\Omega_k}^2 \lesssim \log^2(d/h) \|\tilde{\mathbf{v}}_h\|_{1, \Omega_k}^2.$$

Substituting this into (4.35) and using (4.34), yields

$$\begin{aligned} \sum_V \|\tilde{\mathbf{v}}_V\|_A^2 &\lesssim \sum_V \sum_{k \in \Lambda_V} \lambda_k \log^2(d/h) \|\tilde{\mathbf{v}}_h\|_{1, \Omega_k}^2 \\ &\lesssim \log^2(d/h) \|\tilde{\mathbf{v}}_h\|_{H_\lambda^1(\Omega)}^2 \\ &\lesssim \log(1/d) \log^2(d/h) \|\mathbf{v}_h\|_A^2. \end{aligned}$$

This, together with (4.33), verify the assumptions of Theorem 4.1 with $C(h, d) = \log(1/d) \log^2(d/h)$. \square

5. NUMERICAL EXPERIMENTS

In this section, we report some numerical results for the linear elasticity problems and Maxwell's equations to illustrate the efficiency of the proposed substructuring methods.

In our experiments, we choose the domain $\Omega = (0, 1)^3$ and define domain decomposition and finite element partition as follows. At first, we divide the domain into n^3 smaller cubes $\Omega_1, \Omega_2 \cdots \Omega_N$, which have the same length d of edges, i.e., $d = 1/n$. We require that $D \subset \Omega$ is just the union of some subdomains in $\{\Omega_k\}$, which yields the desired domain decomposition. Next, we divide each subdomain Ω_k into m^3 fine cubes, with the same size $h = 1/(mn)$. Then we further divide each fine cube into 5 or 6 tetrahedrons in the standard way, then all the generated tetrahedrons constitute a partition \mathcal{T}_h consisting of tetrahedral elements.

We discretize the models by the linear finite element methods, and we apply the PCG method with the proposed preconditioner to solve the resulting algebraic systems. The PCG iteration is terminated in our experiments when the relative residual is less than 10^{-6} . We will report the iteration counts in the rest of this section.

5.1. Tests for linear elasticity problems. In this subsection, we choose the right-hand side \mathbf{f} of system (4.12) such that the analytic solution $\mathbf{u} = (u_1, u_2, u_3)^T$ is given by:

$$\begin{aligned} u_1 &= x(x-1)y(y-1)z(z-1) \\ u_2 &= x(x-1)y(y-1)z(z-1) \\ u_3 &= x(x-1)y(y-1)z(z-1) \end{aligned}$$

where the coefficients $\lambda(x) = \mu(x) = 1$. In our experiments, the right-hand side \mathbf{f} is fixed.

In this part, we test the action of the preconditioner B described by **Algorithm 3.1**. We consider the following different distributions of the coefficients $\lambda(x), \mu(x)$:

Case (i): the coefficients have no jump, i.e., $\lambda(x) = \mu(x) = 1$.

Case (ii): the coefficients have large jumps, i.e.,

$$\lambda(\mathbf{x}) = \begin{cases} \lambda_0, & \text{in } D \\ 1, & \text{in } \Omega \setminus D, \end{cases} \quad \mu(\mathbf{x}) = \begin{cases} \mu_0, & \text{in } D, \\ 1, & \text{in } \Omega \setminus D \end{cases}$$

Hereafter we consider two choices of D :

$$\text{Choice (1). } D = [\frac{1}{4}, \frac{1}{2}]^3; \text{ Choice (2). } D = [\frac{1}{4}, \frac{1}{2}]^3 \cup [\frac{1}{2}, \frac{3}{4}]^3.$$

The iteration counts of the PCG method with B are listed in TABLE 1 (for **Case (i)**) and TABLE 2 (for **Case (ii)**).

TABLE 1

Iteration counts of PCG with the preconditioner B : the coefficients have no jump

$m \setminus n$	4	6	8	10
4	18	19	19	18
8	20	20	20	19
12	22	21	21	20
16	23	23	22	21

TABLE 2

Iteration counts of PCG with the preconditioner B : the coefficients have large jumps

	Choice (1) of D				Choice (2) of D			
	$\lambda_0 = \mu_0 = 10^{-5}$		$\lambda_0 = \mu_0 = 10^5$		$\lambda_0 = \mu_0 = 10^{-5}$		$\lambda_0 = \mu_0 = 10^5$	
$m \setminus n$	4	8	4	8	4	8	4	8
4	16	18	25	22	16	19	25	22
8	17	20	27	23	17	21	27	23
12	19	21	28	24	18	23	28	24
16	20	22	29	25	20	24	29	26

We observe from TABLE 1 that the iteration counts of PCG method grows slowly when $m = d/h$ increases but $n = 1/d$ is fixed, and that these counts vary stably when m is fixed but n increases. This show that, when the coefficients is smooth, the condition number of the preconditioned system $B^{-1}A$ should grow logarithmically with d/h only, not depend on $1/d$. The data in TABLE 2 indicate that, even if the coefficients have large jumps, the iteration counts of PCG still grows slowly. It confirms that the preconditioner B is effective for the system arising from nodal element discretization for linear elasticity problems.

5.2. Tests for Maxwell's equations. In this subsection, we consider Maxwell's equations. For the time-dependent Maxwell's equations, we need to solve the following **curlcurl**-system at each time step (see [6, 26, 43]):

$$\begin{cases} \mathbf{curl}(\alpha \mathbf{curl} \mathbf{u}) + \beta \mathbf{u} = \mathbf{f}, & \text{in } \Omega, \\ \mathbf{u} \times \mathbf{n} = 0, & \text{on } \partial\Omega \end{cases} \quad (5.1)$$

where the coefficients $\alpha(\mathbf{x})$ and $\beta(\mathbf{x})$ are two positive bounded functions in Ω . \mathbf{n} is the unit outward normal vector on $\partial\Omega$.

Let $H(\mathbf{curl}; \Omega)$ be the Sobolev space consisting of all square integrable functions whose **curl**'s are also square integrable in Ω , and $H_0(\mathbf{curl}; \Omega)$ be a subspace of $H(\mathbf{curl}; \Omega)$ of all functions whose tangential components vanishing on $\partial\Omega$. In an analogous way, in order to get the weak form of (5.1), just like linear elasticity problems, let $V(\Omega) = H_0(\mathbf{curl})$, and

$$\begin{aligned} \mathcal{A}(\mathbf{u}, \mathbf{v}) &= \int_{\Omega} (\alpha \mathbf{curl} \mathbf{u} \cdot \mathbf{curl} \mathbf{v} + \beta \mathbf{u} \cdot \mathbf{v}) dx, \\ \langle \mathbf{F}, \mathbf{v} \rangle &= \int_{\Omega} \mathbf{f} \cdot \mathbf{v} dx. \end{aligned}$$

Let $R(K)$ be a subset of all linear polynomials on the element K of the form:

$$R(K) = \left\{ \mathbf{a} + \mathbf{b} \times \mathbf{x}; \mathbf{a}, \mathbf{b} \in \mathbb{R}^3, \mathbf{x} \in K \right\}.$$

It is well-known that for any $\mathbf{v} \in V_h(\Omega)$, its tangential components are continuous on all edges of each element in the triangulation \mathcal{T}_h . Moreover, each edge element function \mathbf{v} in $V_h(\Omega)$ is uniquely determined by its moments on each edge e of \mathcal{T}_h :

$$\left\{ \lambda_e(\mathbf{v}) = \int_e \mathbf{v} \cdot \mathbf{t}_e ds; e \in \mathcal{E}_h \right\}, \quad (5.2)$$

where \mathbf{t}_e denotes the unit vector on the edge e .

As in the last subsection, we assume that Ω can be written as the union of polyhedral subdomains D_1, \dots, D_{N_0} with N_0 being a fixed positive integer, such that $\alpha(x) = \alpha_r$ and $\beta(x) = \beta_r$ for $x \in D_r$, where every α_r and β_r is a positive constant. Let the subdomains Ω_k satisfy the condition: each D_r is the union of some subdomains in $\{\Omega_k\}$.

Let the right-hand side \mathbf{f} in the equations (5.1) to be selected such that the exact solution $\mathbf{u} = (u_1, u_2, u_3)^T$ is given by

$$\begin{aligned} u_1 &= xyz(x-1)(y-1)(z-1), \\ u_2 &= \sin(\pi x) \sin(\pi y) \sin(\pi z), \\ u_3 &= (1 - e^x)(1 - e^{x-1})(1 - e^y)(1 - e^{y-1})(1 - e^z)(1 - e^{z-1}), \end{aligned}$$

where the coefficients $\alpha(\mathbf{x})$ and $\beta(\mathbf{x})$ are both constant 1. This right-hand side \mathbf{f} is also fixed in our experiments.

In this part, we investigate the effectiveness of the preconditioner B described by **Algorithm 3.1**. We consider the following different distributions of the coefficients $\alpha(\mathbf{x})$ and $\beta(\mathbf{x})$:

Case (i): the coefficients have no jump, i.e., $\alpha(\mathbf{x}) = \beta(\mathbf{x}) = 1$.

Case (ii): the coefficients have large jumps, i.e.,

$$\alpha(\mathbf{x}) = \begin{cases} \alpha_0, & \text{in } D \\ 1, & \text{in } \Omega \setminus D, \end{cases} \quad \beta(\mathbf{x}) = \begin{cases} \beta_0, & \text{in } D, \\ 1, & \text{in } \Omega \setminus D \end{cases}$$

The iteration counts of the PCG method with B are listed in TABLE 3 (for **Case (i)**) and TABLE 4 (for **Case (ii)**).

TABLE 3

Iteration counts of PCG with the preconditioner B : the coefficients have no jump

$m \setminus n$	4	6	8	10
4	16	16	15	15
8	18	17	17	16
12	19	19	18	18
16	20	20	19	19

TABLE 4

Iteration counts of PCG with the preconditioner B : the coefficients have large jumps

	Choice (1) of D				Choice (2) of D			
	$\beta_0 = \alpha_0 = 10^{-5}$		$\beta_0 = \alpha_0 = 10^5$		$\beta_0 = \alpha_0 = 10^{-5}$		$\beta_0 = \alpha_0 = 10^5$	
$m \setminus n$	4	8	4	8	4	8	4	8
4	14	15	19	18	13	16	18	19
8	15	17	21	20	15	17	21	21
12	16	19	23	21	16	19	22	23
16	17	20	24	22	17	20	24	24

We observe from the above two tables that, although the coarse space is chosen as the simplest one for Maxwell’s equations, the iteration counts of the PCG method with the preconditioner B grow logarithmically with $m = d/h$ only, not depend on $n = 1/d$, even if the coefficients have large jumps.

5.3. Numerical results on irregular subdomains. In this subsection, we consider the case of irregular subdomains explained in Subsection 3.4. As usual (refer

to [13]), here we consider only the case with constant coefficient 1 (if the coefficients have large jumps, we can not require that the distribution of the jumps of the coefficients is consistent with that of the irregular subdomains).

We still use N to denote the number of subdomains (which are not cubes any more) and h to denote the fine mesh size.

Firstly, we consider the domain Ω is a unit cube (see FIGURE 2). We do the experiments for both linear elasticity problems and Maxwell's equations. In order to describe the results clearly, we use the previous symbols m and n . Here $n = \sqrt[3]{N}$ and $m = \frac{1}{h\sqrt[3]{N}}$. In TABLE 5, we list the iteration counts of PCG method with the proposed preconditioner.

TABLE 5
Iterations counts of PCG method with the preconditioner B for irregular subdomain partition on cubic domain

Maxwell's equations				
$m \setminus n$	4	6	8	10
4	21	21	21	22
8	23	24	22	24
12	25	25	25	25
16	27	26	27	26
Linear elasticity problems				
$m \setminus n$	4	6	8	10
4	24	23	24	23
8	28	29	27	29
12	30	32	33	32
16	32	33	33	34

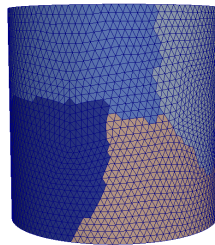


FIGURE 4. irregular partition for Ω

Secondly, we consider the standard cylinder domain. The mesh partition and subdomains are shown in FIGURE 4. We use N_e to denote the total number of elements of fine mesh. We test two series of mesh: $N_e = 765952$ and $N_e = 6127616$. Here $n = \sqrt[3]{N}$ and $m \approx \sqrt[3]{\frac{N_e}{N}}$. The iteration counts of PCG are listed in TABLE 6.

TABLE 6
Iterations counts of PCG method with the preconditioner B for irregular subdomain partition on cylindrical domain

Maxwell's equations							
$m \setminus n$	4	$m \setminus n$	6	$m \setminus n$	8	$m \setminus n$	10
23	24	15	23	11	22	9	22
46	23	31	23	23	26	18	23
Linear elasticity problem							
$m \setminus n$	4	$m \setminus n$	6	$m \setminus n$	8	$m \setminus n$	10
23	28	15	26	11	24	9	25
46	39	31	32	23	29	18	27

The above two tables indicate that, even if the subdomains are irregular, the proposed preconditioner is still effective. We point out that the dimensions of the coarse space in the current situation have not obvious increase comparing with the case with regular subdomains considered in previous two subsections.

5.4. Comparison with the BDDC method. In this part, we compare the proposed method with the BDDC method. All our codes run in sequential way, except when coarse problem and local problems are solved by direct solver package MUMPS, in which high performance OpenBLAS libraries based on multithreading parallelism are called. In TABLE 7, we list the PCG iteration counts and the running time for the linear elasticity problems and in TABLE 8, 9 for Maxwell's equations. Here we use B and \tilde{B} to denote the preconditioners with exact vertex-related solvers B_V and with inexact one \tilde{B}_V , respectively.

In order to shorten the length of the paper, in TABLE 7 we only list the results for $\lambda_0 = \mu_0$ and regular subdomain partition. The parameters m and n are the same meaning as in TABLE 2. As mentioned in [11], when using corner constraints only, we get bad performance in the BDDC method. Because of this, in TABLE 7 we consider both corner and edge constraints for the BDDC method.

TABLE 7
Iteration counts and time(s) for the linear elasticity problems: Choice (2) of D , $\lambda_0 = \mu_0$ and regular partition on cubic domain

λ_0	$m = n$	BDDC				B				\tilde{B}			
		iter	setup	solve	total	iter	setup	solve	total	iter	setup	solve	total
10^5	4	7	0.6	0.1	0.7	25	0.4	0.2	0.6	25	0.3	0.2	0.5
	8	11	52.2	10.5	62.7	23	24.6	19.8	44.4	25	16.7	14.4	31.1
	12	14	696.6	179.1	875.7	24	406.8	290.8	697.6	26	256.0	221.4	477.4
1	4	7	0.5	0.1	0.6	18	0.4	0.2	0.6	19	0.3	0.1	0.4
	8	10	57.4	11.3	68.7	20	25.4	17.2	42.6	21	16.5	12.2	28.7
	12	13	734.1	167.3	901.4	20	356.5	244.4	600.9	22	254.0	189.9	443.9
10^{-5}	4	7	0.6	0.1	0.6	16	0.4	0.1	0.5	16	0.3	0.1	0.4
	8	11	52.9	10.6	63.5	21	24.7	18.1	42.8	23	17.6	13.3	30.9
	12	13	716.1	167.2	883.3	23	364.7	286.0	650.7	26	255.2	219.0	474.2

It can be seen from TABLE 7 that the BDDC preconditioner has the smallest PCG iteration counts among all the tested preconditioners. However, one has to solve algebraic equations to get coarse basis functions in the BDDC method. As mentioned in the existing works, if only corner constraints are used, the iteration counts varies unstably for the BDDC method. When edges and corner constraints are used, one needs to solve local saddle-point problem 60 times for each floating subdomain in the BDDC method. In addition, the adding constraints to local problems enlarge the size of local problems for BDDC method. This can explain why the total CPU time for setting-up in the BDDC method is more than that in the proposed method. Due to these reasons, the proposed method has less cost than the BDDC method.

As for Maxwell's equations, we list the results in TABLE 8 for regular subdomain partition and in TABLE 9 for irregular subdomain partition. As mentioned in [13], instead of using deluxe scaling, we use e-deluxe scaling in BDDC method, which can result in significant computational savings and indistinguishable iteration counts.

TABLE 8

Iteration counts and time(s) for Maxwell's equation: $\beta = 1$ and regular partition on cubic domain

α	$n = m$	BDDC				B				\tilde{B}			
		iter	setup	solve	total	iter	setup	solve	total	iter	setup	solve	total
10^3	4	9	0.8	0.4	1.2	17	0.7	0.4	1.1	19	0.6	0.5	1.1
	8	12	73.7	25.3	99.0	19	45.0	36.6	81.6	21	32.8	27.4	59.2
	10	13	337.7	106.8	444.5	19	193.8	148.1	341.9	21	137.4	122.8	260.2
10^2	4	9	0.8	0.3	1.1	17	0.6	0.4	1.0	19	0.7	0.5	1.1
	8	12	62.5	24.5	87.0	18	44.3	34.3	78.7	21	33.2	28.4	61.6
	10	13	291.6	111.7	403.3	19	192.5	158.8	351.3	21	138.5	123.8	262.5
1	4	9	0.9	0.3	1.2	16	0.7	0.4	1.1	18	0.7	0.5	1.2
	8	12	62.7	24.9	87.6	17	49.0	37.1	86.1	19	33.3	24.5	57.8
	10	12	296.8	102.5	399.3	18	198.5	154.1	352.6	19	138.5	112.2	250.7
10^{-4}	4	9	0.8	0.3	1.1	11	0.6	0.3	0.9	18	0.6	0.4	1.0
	8	12	64.0	24.9	88.8	11	47.1	21.0	68.10	17	32.1	21.7	53.8
	10	13	296.8	102.5	399.3	11	198.5	154.1	352.6	19	138.5	112.2	250.7
10^{-6}	4	13	0.8	0.5	1.3	11	0.7	0.3	1.0	20	0.5	0.5	1.0
	8	19	75.7	38.4	114.1	9	46.5	16.3	62.8	22	32.0	28.4	60.4
	10	20	274.2	152.9	427.1	9	192.9	74.7	267.6	17	140.9	98.8	239.7

In the case of regular subdomain partition, for each floating cubic subdomain, one needs to solve local saddle-point problems 24 times to get coarse basis functions in the BDDC method. Because of this, the results in TABLE 8 indicate that the setting up time of BDDC method is larger than the proposed method. Then the total time of BDDC method is larger than the proposed methods although its iteration counts is smaller than our method. When solving B_V in inexact manner, we can further save much time than B in the setting up phase. From TABLE 8, we observed that the preconditioner \tilde{B} has faster convergence than the BDDC preconditioner. We know that, if $\alpha/\beta \ll 1$, the operator A has very good conditioning. But, we found a surprising phenomenon: when increasing the value of m , the iteration counts of the BDDC method grows quickly and is larger than the proposed method.

TABLE 9

Iteration counts and time(s) for Maxwell's equation: $\beta = 1$ and irregular partition on cubic domain

		BDDC				B			
α	$n = m$	iter	setup	solve	total	iter	setup	solve	total
10^3	4	13	1.6	1.4	3.0	23	1.1	0.8	1.9
	8	18	112.6	75.5	188.1	25	69.7	51.6	121.3
	10	20	418.9	252.8	671.7	27	293.9	184.4	478.3
10^2	4	13	1.7	1.5	3.1	23	1.0	0.8	1.8
	8	18	114.8	75.4	190.2	24	69.0	49.5	118.5
	10	20	421.4	249.3	670.7	26	296.0	177.9	473.9
1	4	13	1.6	1.4	3.0	21	1.0	0.7	1.7
	8	18	111.8	75.2	187.0	22	68.8	45.9	114.7
	10	20	417.7	254.8	672.5	24	299.5	165.7	465.2
10^{-4}	4	11	1.6	1.3	2.9	13	1.1	0.5	1.6
	8	15	113.3	63.6	177.0	13	69.4	26.9	97.3
	10	19	422.6	238.6	661.2	14	293.5	97.9	391.4
10^{-6}	4	12	1.6	1.3	2.9	14	1.1	0.5	1.5
	8	21	113.5	87.5	201.0	12	69.3	26.8	96.1
	10	28	420.6	343.7	764.2	11	293.9	77.8	371.7

In TABLE 9, the parameters m and n have the same meanings as in TABLE 5. We observed that both setting up time and PCG solving time in the proposed method are less than that in the BDDC method. Since the geometric properties of subdomains generated by Metis are very complicated, the number of subdomain edges on each irregular subdomain may be much larger than the one in a cubic subdomain and so the total subdomain edges is much larger than the regular subdomain partition case. The drawback in irregular subdomain partition enlarges the size of local saddle-point problems and increase the cost of calculation for e-deluxe scaling operator. This investigation can explain why the PCG solving time in the BDDC method is also larger than that in the proposed method. For the case with irregular subdomains, we have not tested the preconditioner \tilde{B} with coarsening technique since the existing coarsening software is not practical yet. In near future, we will try to design special coarsening software for irregular subdomains.

6. CONCLUSION

In this paper, we have constructed one substructuring preconditioner with the simplest coarse space for general elliptic-type problems in three dimensions. In particular, we design new local interface solvers, which are easy to implement and

do not depend on the considered models. The proposed preconditioner can absorb some advantages of the non-overlapping and overlapping domain decomposition methods. We have given an analysis of convergence of the preconditioner for linear elasticity problems, which shows the proposed preconditioner is nearly optimal and also robust with respect to the (possibly large) jumps of the coefficient. We also consider the case with irregular subdomain partition for numerical experiments. We have given some numerical results to show that the proposed preconditioner is effective uniformly for the linear elasticity problem and Maxwell's equations in three dimensions.

REFERENCES

- [1] J. Bramble, J. Pasciak and A. Schatz, The construction of preconditioners for elliptic problems by substructuring, IV. *Math. Comp.*, **53**(1989), pp.1-24.
- [2] S. Brenner and L. Sung, BDDC and FETI-DP without matrices or vectors, *Comput. Methods Appl. Mech. Engrg.*, **196**(2007), 1429-1435.
- [3] X. Cai, An additive Schwarz algorithms for parabolic convection-diffusion equation, *Numer. Math.*, **60**1991, No.1, pp.41-61
- [4] X. Cai, The use of pointwise interpolation in domain decomposition methods with nonnested meshes, *SIAM J. Sci. Comput.*, **16**(1995), pp. 250-256.
- [5] X. Cai and M. Sarkis, A Restricted additive Schwarz preconditioner for general sparse linear system, *SIAM J. Sci. Comput.*, **21**(1999), No. 2, pp. 792-797, Springer-Verlag, Berlin, Heidelberg, New York, 2008. Third edition.
- [6] M. Cessenat. *Mathematical methods in electromagnetism*. World Scientific, River Edge, NJ, 1998.
- [7] T. Chan and J. Zou, Additive Schwarz domain decomposition methods for elliptic problems on unstructured meshes, *Numer. Algorithms*, **8**(1994), pp. 329-346.
- [8] T. Chan, B. Smith, and J. Zou. Overlapping Schwarz methods on unstructured meshes using non-matching coarse grids. *Numer. Math.*, **73**(2):149-167, 1996.
- [9] X. Chen and Q. Hu, Inexact solvers for saddle-point system arising from domain decomposition of linear elasticity problems in three dimensions. *International Journal of Numerical Analysis & Modeling*, **8**(2011), No. 1, p156-173.
- [10] E. Chung, H. Kim, and O. Widlund. Two-Level Overlapping Schwarz Algorithms for a Staggered Discontinuous Galerkin Method, *SIAM J. Numer. Anal.* **51**(2013), No.1, 47-67.
- [11] C. Dohrmann, A preconditioner for substructuring based on constrained energy minimization, *SIAM J. Sci. Comput.* vol.25, No. 1, pp. 246-258, 2003.
- [12] C. Dohrmann and O. Widlund, An Iterative Substructuring Algorithm for Two-Dimensional Problems in $H(\text{curl})$, *SIAM J. Numer. Anal.* **50**(2012), No.3, pp.1004-1028.
- [13] C. Dohrmann and O. Widlund, A BDDC Algorithm with Deluxe Scaling for Three-Dimensional $H(\text{curl})$ Problems, *Comm. Pure Appl. Math.*, 2015, doi: 10.1002/cpa.21574
- [14] M. Dryja, J. Galvis, and M. Sarkis, BDDC methods for discontinuous Galerkin discretization of elliptic problems, *J. Complexity*, **23**(2007), 715-739.
- [15] M. Dryja, F. Smith and O. Widlund, Schwarz analysis of iterative substructuring algorithms for elliptic problems in three dimensions, *SIAM J. Numer. Anal.* **31**(1994), No.6, pp.1662-1694
- [16] M. Dryja, O. B. Widlund, Domain decomposition algorithms with small overlap, *SIAM J. Sci. Comput.*, **15**(1994), pp. 604-620.

- [17] M. Dryja and O. Widlund, Schwarz methods of Neumann-Neumann type for three-dimensional elliptic finite element problems, *Comm. Pure Appl. Math.*, 48 (1995), pp. 121-155.
- [18] O. Dubois and M. Gander, Optimized Schwarz methods for a diffusion problem with discontinuous coefficient, to appear in *Numerical Algorithms*
- [19] C. Farhat and F. Roux, A method of finite element tearing and interconnecting and its parallel solution algorithm, *Internat. J. Numer. Methods Engrg.*, 32 (1991), pp. 1205-1227.
- [20] C. Farhat, M. Lesoinne, and K. Pierson, A scalable dual-primal domain decomposition method, *Numer. Linear Algebra Appl.*, 7 (2000), pp. 687-714.
- [21] C. Farhat, J. Mandel, and F. Roux, Optimal convergence properties of the FETI domain decomposition method, *Comput. Methods. Appl. Mech. Engrg.*, 115 (1994), pp. 365-388
- [22] A. Frommer and D. Szyld, An algebraic convergence theory for restricted additive Schwarz methods using weighted max norms, *SIAM J. Numer. Anal.*, 39 (2001), pp. 463-479.
- [23] M. Gander, Optimized Schwarz Methods, *SIAM J. Numer. Anal.*, **44**(2006), No. 2, pp. 699-731
- [24] M. Gander and F. Kwok, Best Robin parameters for optimized Schwarz methods at cross points, *SIAM J. Sci. Comput.*, 34 (2012), pp. 1849-1879.
- [25] C. Geuzaine and J.-F. Remacle, Gmsh: a three-dimensional finite element mesh generator with built-in pre- and post-processing facilities.
- [26] R. Hiptmair. Finite elements in computational electromagnetism. *Acta Numerica*, 11:237-339, 2002.
- [27] Q. Hu, Z. Shi and D. Yu, Efficient solvers for saddle-point problems arising from domain decompositions with Lagrange multipliers, *SIAM J. Numer. Anal.*, 42(2004), no. 3, 905-933.
- [28] Q. Hu, A Regularized Domain Decomposition Method with Lagrange Multiplier, *Adv Comput Math*, Vol. 26, No. 4. (May 2007), pp. 367-401
- [29] Q. Hu, S. Shu And J. Wang, Nonoverlapping domain decomposition methods with a simple coarse space for elliptic problems. *Math.Comput.*, **79**(2010), No.272, pp.2059-2078
- [30] Q. Hu, S. Shu and J. Zou. A substructuring preconditioner of three-dimensional Maxwell's equations, in *Domain Decomposition Methods in Science and Engineering XX* (No. 91 in *Lecture Notes in Computational Science and Engineering*), pages 73-84, edited by R. Bank, M. Holst, O. Widlund and J. Xu, Heidelberg-Berlin, 2013. Springer. Proceedings of the Twentieth International Conference on Domain Decomposition Methods, held at the University of California at San Diego, CA, February 9-13, 2011.
- [31] Q. Hu and J. Zou. A nonoverlapping domain decomposition method for Maxwells equations in three dimensions. *SIAM J. Numer. Anal.*, 41(5):1682-1708, 2003.
- [32] Q. Hu and J. Zou. Substructuring preconditioners for saddle-point problems arising from Maxwells equations in three dimensions. *Math. Comp.*, **73**(245):35-61 (electronic), 2004.
- [33] Peter W. Jones. Quasiconformal mappings and extendability of functions in Sobolev space. *Acta Math.*, 147(1-2):71-88, 1981.
- [34] George Karypis. METIS, A Software Package for Partitioning Unstructured Graphs, Partitioning Meshes, and Computing Fill-Reducing Orderings of Sparse Matrices, Version 5.1.0. University of Minnesota, Department of Computer Science and Engineering, Minneapolis, MN, 2013.
- [35] A. Klawonn, O. B. Widlund, A domain decomposition method with Lagrange multipliers and inexact solvers for linear elasticity, *SIAM J. Sci. Comput.*, 22(2000) 1199-1219.
- [36] A. Klawonn, O. Widlund and M. Dryja, Dual-Primal FETI methods for three-dimensional elliptic problems with Heterogeneous coefficients. *SIAM J. Numer. Anal.*, 40(2002), 159-179.
- [37] A. Klawonn, O. Rheinbach, and O. B. Widlund, An analysis of a FETI-DP algorithm on irregular subdomains in the plane, *SIAM J. Numer. Anal.*, 46 (2008), pp. 2484-2504.

- [38] H. Kim and X. Tu, A three-level BDDC algorithm for mortar discretizations, *SIAM J. Numer. Anal.*, **47**(2009), 1576-1600.
- [39] J. Li and O. Widlund, On the use of inexact subdomain solvers for BDDC algorithms, *Comput. Methods Appl. Mech. Engrg.*, **196**(2007), 1415-1428.
- [40] J. Mandel and M. Brezina, Balancing domain decomposition for problems with large jumps in coefficients, *Math. Comput.*, 65 (1996), pp. 1387-1401.
- [41] J. Mandel and C. Dohrmann, Convergence of a balancing domain decomposition by constraints and energy minimization, *Numer. Linear Algebra Appl.*, 2003.
- [42] J. Mandel, C. Dohrmann and R. Tezaur. An algebraic theory for primal and dual substructuring methods by constraints. *Appl. Numer. Math.*, **54**(2005), 167-193.
- [43] P. Monk. *Finite Element Methods for Maxwells Equations*. Oxford University Press, Oxford, 2003.
- [44] J. Nécas, *Les méthodes directes en théorie des équations elliptiques*, Academia, Prague, 1967.
- [45] Hang Si. *TetGen, A Quality Tetrahedral Mesh Generator and 3D Delaunay Triangulator*, Version 1.5.
- [46] B. Smith. An optimal domain decomposition preconditioner for the finite element solution of linear elasticity problems. *SIAM Journal on Scientific and Statistical Computing*, **13**(1992), No.1, pp.364-378.
- [47] Andrea Toselli. Overlapping Schwarz methods for Maxwells equations in three dimensions. *Numer. Math.*, 86:733-752, 2000.
- [48] Andrea Toselli. Dual-primal FETI algorithms for edge finite element approximations in 3D. *IMA J. Numer. Anal.*, 26:96-130, 2006.
- [49] A. Toselli, O. Widlund. *Domain decomposition methods: algorithms and theory*. Berlin: Springer, 2005.
- [50] L. Veiga, D. Cho, L. Pavarino, S. Scacchi, Overlapping Schwarz methods for Isogeometric Analysis, *SIAM J. Numer. Anal.*, **50**(2012), 1394-1416.
- [51] L. Veiga, L. Pavarino, S. Scacchi, O. Widlund and S. Zampini, Isogeometric BDDC Preconditioners with Deluxe Scaling, *SIAM J. Sci. Comput.*, 36(2014), No. 3, pp. 1118-1139
- [52] J. Xu and Y. Zhu, Uniform convergent multigrid methods for elliptic problems with strongly discontinuous coefficients, *M3AS*, 18(2008), 77-105.
- [53] J. Xu and J. Zou, *Some non-overlapping domain decomposition methods*, *SIAM Review*, **24**(1998)